Interrogating the role of arginine methyltransferases in radiation response in glioma

by

Beyza Nur Köseoğlu

A Dissertation Submitted to the

Graduate School of Sciences and Engineering

in Partial Fulfillment of the Requirements for

the Degree of

Master of Science

in

Cellular and Molecular Medicine

KOÇ UNIVERSITY

January, 2024

Koç University

Graduate School of Sciences and Engineering

This is to certify that I have examined this copy of a master's thesis by

Beyza Nur Köseoğlu

and have found that it is complete and satisfactory in all respects,

and that any and all revisions required by the final

examining committee have been made.

Committee Members:

Prof. Dr. Tuğba Bağcı-Onder (Advisor)

Assoc. Prof. Tolga Emre

Prof. Dr. Kemal Baysal

Date: _____

I dedicate my thesis,

to my family

ABSTRACT

Interrogating the role of arginine methyltransferases in radiation response in glioma

Beyza Nur Köseoğlu

Master of Science in Cellular and Molecular Medicine

30 January, 2024

Radiotherapy (RT) is an important survival-prolonging treatment for glioblastoma (GBM), a largely incurable primary malignant brain tumor. The treatment failure relies on the adaptation of tumor cells to treatment and resistance, which is a major reason for inevitable recurrence. Understanding the molecular mechanisms behind this adaptive resistance and designing effective therapeutic strategies are of utmost priority. Therefore, finding epigenetic modulators of RT response, in other words, "radiosensitizers", is crucial for GBM patients.

This thesis investigates the effects of Arginine methyltransferase family (PRMT) inhibition on the RT response of glioblastoma cells. PRMTs are among histone-modifying enzymes, which provides methylation of arginine residues on histones, thereby regulating transcriptional activity. While PRMTs have been functionally implicated in cancer and there is a considerable effort for various PRMT inhibitors as anti-cancer drugs, combinatorial effects of PRMT inhibitors and RT have not been well-characterized in GBM. Our interest in PRMT inhibitors stems from our lab's previously conducted unbiased chemical screen with epigenetic drugs, which identified several PRMT inhibitors as radiosensitizers in GBM cells. In this thesis, this finding was further explored in detail. First, effects of PRMT inhibitors as single agents were tested on GBM cell lines and optimal doses of drugs were selected to be further explored. To assess the combined efficacy of PRMT inhibitors and RT, cell viability analyses were conducted on U373 GBM cells treated with various radiation doses and various PRMT inhibitors (MS023, MS049, SGC707, and LLY283). Particularly, the drug MS023, targeting the Type-I PRMT family, exhibited a significant impact on survival and reduced proliferation capacity of GBM cells when combined with RT. Additionally, as a complement to the chemical approach, CRISPR/Cas9-based genetic ablation was employed to reduce the expression of genes encoding relevant PRMT enzyme family members. The combined effect

of PRMT inhibition and RT was comprehensively examined through these diverse experimental approaches.

In the subsequent stage of the thesis, the molecular mechanisms underlying the relationship between PRMT inhibition and RT response were explored by using RNA sequencing and the effects of MS023 and ionizing radiation on the transcriptome of GBM cells were defined. The results indicate that PRMT inhibition modulates the expression of genes related to the functioning of cell cycle and mitosis, which may partly account for the radiosensitization potential of these drugs in GBM.

These findings establish a foundational framework for identifying RT resistance mechanisms and devising innovative combination therapy strategies tailored for GBM. The observed effects of PRMT inhibition on RT response offer promising avenues for future research and potential clinical applications.

ÖZETÇE

Arginin metiltransferazların gliomda radyasyon yanıtındaki rolününün incelenmesi

Beyza Nur Köseoğlu

Hücresel ve Moleküler Tıp, Yüksek Lisans

30 Ocak, 2024

Radyoterapi (RT), genellikle tedavisi zor bir primer malign beyin tümörü olan glioblastoma (GBM) için önemli bir hayatta kalma süresini uzatan bir tedavidir. Tedavi başarısızlığı, tümör hücrelerinin tedaviye ve dirence adapte olmasına dayanmakta olup, bu, kaçınılmaz nüksün ana nedenlerinden biridir. Bu adaptif direncin moleküler mekanizmalarını anlamak ve etkili terapötik stratejiler tasarlamak son derece önceliklidir. Bu nedenle, RT yanıtındaki epigenetik modülatörleri, yani "radyosenzitizörleri" bulmak, GBM hastaları için hayati öneme sahiptir.

Bu tez, Arginin metiltransferaz ailesinin (PRMT) inhibitörlerinin glioblastoma hücrelerinin RT yanıtı üzerindeki etkilerini araştırmaktadır. PRMT'ler, histonlar üzerinde metilasyon gerçekleştirerek histon modifikasyon enzimleri arasında yer alır ve bu şekilde transkripsiyonel aktiviteyi düzenler. PRMT'ler kanserle işlevsel olarak ilişkilendirilmiş olmalarına rağmen ve çeşitli PRMT inhibitörleri antikanser ilaçlar olarak kullanılmak üzere yoğun bir çaba gösterilmekteyken, PRMT inhibitörlerinin ve RT'nin kombinasyonel etkileri GBM'de iyi karakterize edilmemiştir. Laboratuvarımızın önceki epigenetik ilaçlarla yapılan kimyasal tarama sonucunda, GBM hücrelerinde birkaç PRMT inhibitörünü radyosenzitizör olarak tanımlamıştır. Bu tezde, bu bulgu daha ayrıntılı bir şekilde incelenmiştir. İlk olarak, PRMT inhibitörlerinin tek başlarına ajan olarak GBM hücre hatları üzerindeki etkileri test edilmiş ve ilaçların daha fazla incelenmesi için optimal dozlar seçilmiştir. PRMT inhibitörlerinin ve RT'nin birlikteki etkinliğini değerlendirmek için, U373 GBM hücreleri üzerinde çeşitli radyasyon dozları ve çeşitli PRMT inhibitörleri (MS023, MS049, SGC707 ve LLY283) ile yapılan hücre canlılığı analizleri gerçekleştirilmiştir. Özellikle, Tip-I PRMT ailesine yönelik olan MS023 adlı ilaç, RT ile birleştirildiğinde GBM hücrelerinin yaşamını önemli ölçüde etkilemiş ve proliferasyon kapasitesini azaltmıştır. Kimyasal yaklaşımın bir tamamlayıcısı olarak, ilgili PRMT enzim aile üyelerini kodlayan genlerin ekspresyonunu azaltmak için CRISPR/Cas9 tabanlı genetik ablasyon da kullanılmıştır. PRMT inhibisyonu

ve RT'nin birleşik etkisi, bu çeşitli deneysel yaklaşımlar aracılığıyla kapsamlı bir şekilde incelenmiştir.

Tezin sonraki aşamasında, PRMT inhibisyonu ile RT yanıtı arasındaki ilişkinin moleküler mekanizmaları, RNA dizileme kullanılarak araştırılmış ve GBM hücrelerinin transkriptomu üzerindeki MS023 ve iyonlaştırıcı radyasyonun etkileri tanımlanmıştır. Sonuçlar, PRMT inhibisyonunun hücre döngüsü ve mitozun işleyişi ile ilgili genlerin ekspresyonunu modüle ettiğini göstermektedir, bu da bu ilaçların GBM'de radyosenzitizasyon potansiyelinin kısmen nedeni olabilir.

Bu bulgular, RT direnç mekanizmalarını tanımlamak ve GBM için özel olarak tasarlanmış yenilikçi kombinasyon terapi stratejileri geliştirmek için temel bir çerçeve oluşturuyor. PRMT inhibisyonunun RT yanıtındaki gözlemlenen etkiler, gelecekteki araştırmalar ve potansiyel klinik uygulamalar için umut verici yollar sunmaktadır.

ACKNOWLEDGEMENTS

I extend my deepest gratitude to the individuals who have played a pivotal role in completing this master's thesis.

First and foremost, I am sincerely thankful to my advisor, Tuğba Bağcı Önder, whose invaluable guidance, unwavering support, and insightful feedback have been instrumental throughout every stage of this research. Her expertise and encouragement have significantly shaped the trajectory of this thesis. I am genuinely appreciative of her supportive and constructive mentorship, and I extend my thanks for fostering an environment where I felt like a valuable individual and a motivated researcher through our insightful conversations.

I would also like to express my gratitude to Assoc. Prof. Tolga Emre and Prof. Kemal Baysal, who served on my thesis jury. Their guidance and support throughout my thesis process have been invaluable. I extend my appreciation to Koç University Research Centre for Translational Medicine (KUTTAM) and the Scientific and Technological Research Council of Turkey (TUBITAK) for providing financial support.

Special appreciation is extended to all past and present TBO lab members. Your collaborative and stimulating environment, along with discussions, feedback, and camaraderie, have significantly enriched my academic experience. Throughout my thesis, I have greatly appreciated working with the IR team, Nareg Pınarbaşı-Değirmenci, and Serdar Aksel Çelikkol. I extend my thanks for your support in experimental discussions, overcoming challenges with the radiation device, and assistance in scientific aspects. I am grateful to Ezgi Yağmur Kala for her heartwarming friendship and the support and motivation provided during the thesis writing process. I would also like to express my gratitude to Ebru Yılmaz for being an amazing travel buddy, accompanying me during experiments, and providing experimental support, particularly in primary cell cultures. I also want to thank to Canan Bayraktar for her extensive knowledge in cloning and various topics, as well as her warm friendship and valuable advice. And also, I extend my sincere thanks to Göktuğ Karabıyık, Ahmet Cingöz and Özlem Yedier-Bayram, who patiently stood by my side whenever I needed them. Ipek Kök and Sedef Saraç, I am very grateful for our numerous fun memories and friendship; your sincerity always made me feel better. A special thanks to Beril Esin and Mina Küçüktaş for the enjoyable experiences, trips, and musical car journeys. Our special

motivation and meditation sessions became unforgettable moments for me, and we will definitely do them again. Erdem Ercan, I appreciate your profound scientific discussions and enriching cultural conversations. Thank you for your guidance during the historical sightseeing tours, and our pleasant exchanges. And lastly, I would like to express my gratitude to Melis Selek, who joined us as an undergraduate intern. Her undeniable contribution to our experiments, along with her high talent, self-discipline, and easy adaptability, is commendable. I am confident that she will be successful scientist in the future.

In my academic journey, I want to extend my thanks to the individuals who have been like family to me in Istanbul. Hande Nur Şahin and İrem Sultan Dilbaz, I am deeply thankful for your countless moments of support, being there for me in every challenging situation, and creating beautiful memories together. Your empathy, sacrifice, and friendship mean the world to me. To Cansu Ercan, Altar Özbıyık, and Muhammet Soytürk, I appreciate your sincerity, our heartfelt conversations, and the many valuable contributions you've made, creating many enjoyable and memorable moments that we shared with laughter.

Another person I appreciate so much is Alperen Acarı, who has brought beautiful friendships and different perspectives into my life. He has made significant contributions to both academic and personal development, providing diverse viewpoints. Most importantly, I appreciate him for his motivation towards success. I also want to express my gratitude to Inci Çiftçi for welcoming me with open arms and for her sincere camaraderie. Your unique and brave decisions, as well as your perspective on life, have undoubtedly enriched my journey. Additionally, I appreciate Berkay Bekdemir for his authenticity contributions and enjoyable conversations. I thank Musa Dırak and Ömer Altıntop for both their friendship and assistance in my data analysis. Lastly, I extend my thanks to Melike Doğru and Adeviye Somtaş for their genuine companionship that has spanned over a decade.

I extend my gratitude to my beloved family -my parents, my crazy and sweetly spoiled twin siblings Ahmet and Ahsen - for providing unwavering support. Special thanks to my sister and friend Feyza Nur. Their support has been instrumental in reaching this point, and I appreciate the rest of my family for standing by me at every step and sharing in this journey.

TABLE OF CONTENTS

LIST OF TABLES

LIST OF FIGURES

NOMENCLATURE

53P1	Tumor Suppressor p35-binding protein 1
ATM	Ataxia telangiectasia-mutated
ATP	Adenosine triphosphate
ATR	Ataxia telangiectasia and Rad3-related protein
BBB	Blood-brain barrier
CBP	CREB-binding protein
CCNB2	Cyclin B2
Chk1	Checkpoint kinase 1
CHK2	Checkpoint kinase 2
CTG	Cell Titer-Glo®
D2HG	D-2-hydroxyglutarate
DDR	DNA damage response
DMEM	Dulbecco's Modified Eagle Medium
DPBS	Dulbecco's Phosphate-Buffered Saline
DSB	Double strand break
EGFR	Epidermal growth factor receptor
ERK1/2	Extracellular signal-regulated kinase 1/2
EZH2	Enhancer of zeste homolog 2
FBS	Fetal Bovine Serum
FDA	Food and drug administration
FOXM1	Forkhead Box Protein M1
GBM	Glioblastoma
GCN5	General control non-repressed 5 protein
GO	Gene ontology
GSC	Glioblastoma stem cells

GSEA	Gene set enrichment analysis
Gy	Gray
H2AX	H2A histone family X
HAT	Histone acetyltransferases
HDAC	Histone deacetylases
HKMT	Histone lysine methyltransferases
HR	Homologous recombination
IC50	The half-maximal inhibitory concentration
IDH	Isocitrate dehydrogenase
IR	Ionizing radiation
KDM2A	Lysine-specific demethylase 2A
MDC1	Mediator of DNA damage checkpoint protein 1
MELK	Embryonic leucine-zipper kinase
MGMT	O^6-methylguanine-DNA methyl-transferase
MRE11	Double Strand Break Repair Nuclease
MRN	MRE11-RAD50-NBS1
NBS1	Nijmegen breakage syndrome 1
NEK2	NIMA-related kinase 2
NF-κB	Nuclear factor kappa-light-chain-enhancer of activated B cells
NHEJ	Non-homologous end joining
P53	Tumor protein 53
PARP1	Poly(ADP-ribose) polymerase 1
PRMT	Protein Arginine methyltransferase
PTEN	Phosphatidylinositol 3,4,5-trisphosphate 3-phosphatase
PTM	post-translational modifications
qRT-PCR	Real-Time Quantitative Reverse Transcription PCR
RNF	Ring finger proteins

RPA	Replication protein A
RT	Radiotherapy
SETD2	SET domain containing 2
Smo	Smoothened
SOC	Cytokine signaling
SSB	Single strand break
STAT3	Signal transducer and activator of transcription 3
SWI/SNF	SWItch/Sucrose Non-Fermentable) family
TIP60	Tat interactive protein 60kDa
TMZ	Temozolomide
USP3	Ubiquitin-specific protease 3
UV	Ultraviolet radiation
WHO	World Health Organization
WISP1	Wnt-induced signalling protein 1
γ-H2AX	Phosphorylated H2AX
μM	Micromolar

Chapter 1:**INTRODUCTION**

1.1 Glioblastoma

Glioblastoma (GBM), classified as grade IV astrocytoma according to the World Health Organization (WHO), is the most prevalent and malignant glioma originating in the central nervous system, encompassing more than 60% of primary brain cancer in adults (Hanif et al., 2017). Age-adjusted incidence rates are higher for males, with a 3.97 per 100,000 compared to 2.53 per 1000,000 for females. Based on clinical characteristics, GBMs have been categorized into two groups. Primary GBM arises *de novo* without history and is present at diagnosis as an advanced cancer. This is typically characterized in older patients (average age ~60), and constitutes approximately 90% of cases, accompanied by genetic alterations such as EGFR overexpression, PTEN mutations, and loss of heterozygosity of chromosome 10q. Secondary GBM arises from low-grade astrocytomas and exhibits a better prognosis and increased overall survival (average age ~45). Common genetic alterations in secondary GBM include isocitrate dehydrogenase-1 (IDH1) mutations, TP53 and ATRX mutations, and loss heterozygosity of chromosome 19q (Parsons et al., 2008; Hanif et al., 2017).

Despite extensive clinical and experimental studies exploring treatment alternatives, there has been no significant alteration in the established standard treatment, which consists of maximal safe resection followed by chemotherapy using temozolomide (TMZ) and concurrent radiotherapy (RT) (Wu et al., 2021). While surgical resection alone provides an average survival of around six months, the median survival was determined as 12.1 months with RT alone and 14.6 months with RT plus TMZ in a clinical study conducted on newly diagnosed GBM patients in 2005 (Stupp et al., 2005). Regretfully, the 5-year survival rate is reported to be only 7.2% (Ostrom et al., 2022). The treatment failure is largely caused by tumour cell adaptation to treatment and development of resistance, leading to the inevitable recurrence. Therefore, the development of effective treatment regimens against GBM requires a thorough understanding of the complicated mechanisms of resistance. Another ongoing issue in treating GBM is its high infiltrative nature, making the total resection at the cellular level practically difficult. Unfortunately, the hypoxic region supplies perivascular niches for glioma-initiating cells. The blood-brain barrier (BBB) is a protective boundary

between the circulatory system and the extracellular space of the central nervous system and is a critical barrier for the delivery of chemotherapeutic drugs in the treatment of GBM (Goenka et al., 2021).

1.2 Therapy of Glioblastoma

The current standard of care for newly diagnosed GBM patients is treatment with surgery followed by a combination of the chemotherapeutic agent TMZ and regional fractionated ionizing radiation (IR). No standard of care has been established specifically for recurrent or progressive GBM. For appropriate treatment, an assessment should be undertaken, considering factors such as the patient's age, the location and size of the tumour, the patient's medical history, and prognostic indicators (Fernandes et al., 2017).

1.2.1 Chemotherapy

Chemotherapy is one of main treatments for GBM, typically initiated two to four weeks post-surgery and often concurrently with or shortly after RT. Occasionally, chemotherapy assumes a central role when surgical removal of the tumor is unfeasible. Chemotherapy, using powerful drugs, aims to destroy rapidly dividing cancer cells through various mechanisms of action such as, DNA alkylation, DNA cross-linking, DNA strand breaks, and mitotic spindle disruption (Wen et al., 2021). Chemotherapy for GBM is still limited to a handful of drugs. In 1999, the oral chemotherapy drug TMZ was approved by the FDA for the treatment of anaplastic astrocytoma, and currently, it is still the most commonly used chemotherapeutic drug for GBM. It is a small molecular alkylating agent that directly damages tumours by methylating purine bases in DNA. Its fundamental cytotoxic effect occurs through the forming of O6-methylguanine lesions, leading to apoptosis, autophagy, and cellular senescence. Additionally, TMZ has been found to possess radiosensitizing properties. When administered concurrently with RT, the drug increases the likelihood of radiation-induced DNA double-strand breaks and cell death (Minniti et al., 2009). Lomustine, another alkylating anti-tumour agent, is distinguished by its notable lipophilicity and compact size, facilitating its ability to traverse the BBB and allowing for oral administration. Fotemustine, a closely related drug with a history of application in melanoma treatment, is presently under scrutiny for its efficacy in managing recurrent glioblastoma (Fernandes et al., 2017).

1.2.2 Radiotherapy

The standard treatment of GBM involves surgical resection to remove as much tumor tissue as possible; however, microscopic remnants may persist, leading to tumor recurrence. RT plays a crucial role in addressing these residual cells post-surgery, preventing their proliferation, and eliminating any remaining tumor mass, especially in cases where surgery poses risks or is not feasible. The primary objective of RT is to precisely target tumor lesions with minimal damage to surrounding normal tissues. This precision is crucial for maximizing the therapeutic impact on cancer cells while minimizing adverse effects on healthy tissues. RT functions by utilizing IR, including gamma rays and X-rays, to induce complex chemical alterations within tumor cells. Direct interaction with DNA causes a cascade of damages, including double-strand breaks (DSB), single-strand breaks (SSB), and base lesions or clustered DNA damage. Additionally, RT indirectly triggers the absorption of high-energy wavelengths by surrounding molecules, resulting in the generation of highly reactive free radicals capable of causing further damage to the DNA (Reisz et al., 2014; Gzell et al., 2017).

The unit of radiation dose is the Gray (Gy), representing one joule of energy absorbed per kilogram of matter. In RT, a 1 Gy dose induces about 3000 damaged bases, 1000 SSBs, and 40 DSBs per cell, underscoring the molecular impact of therapeutic radiation (Joubert et al., 2007). Optimal RT dosage, typically delivered at 2 Gy per fraction over six weeks (totaling 60 Gy), has been identified based on studies evaluating tolerability and survival (Barani et al., 2015 & Singh, 2021). Randomized studies underscore the effectiveness of post-surgery RT, surpassing outcomes achieved with chemotherapy or surgery alone.

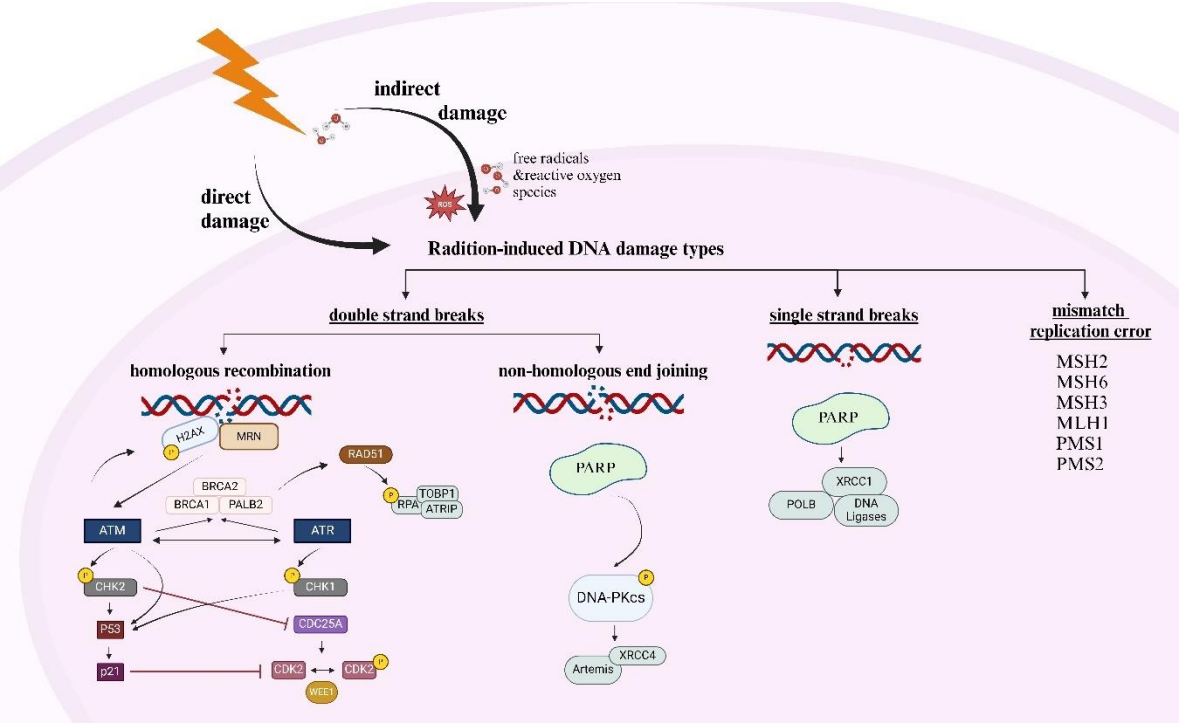

Figure 1.1 Ionizing Radiation-induced DNA Damage Response and Repair Pathways. Figure adapted from (Pilié et al., 2019).

1.3 Therapy Resistance in GBM

Glioblastoma poses a difficult challenge in treatment due to its inherent resistance to conventional therapies. Persistent challenges such as the tumor's proliferative nature, extensive infiltration capacity, and acquired resistance to treatments hinder the effective management of GBM. While radiotherapy plays a crucial role in GBM treatment, the development of cellular resistance to radiation contributes to tumour relapse. Therefore, elucidating the mechanisms responsible for differences in the radiosensitivity of glioma cells becomes paramount for advancing our understanding and improving therapeutic outcomes.

The tumor microenvironment in GBM plays a significant role in the initiation and progression of the disease. Various alterations within this microenvironment contribute to mechanisms and biomolecules influencing the response to radiation. Hypoxia, a critical factor in regulating GBM tumorigenesis, serves as an indicator of poor prognosis (Womeldorff et al., 2014). In the hypoxic tumor microenvironment, disruptions caused by low linear energy transfer radiation provide cells with an extended window for repair and

mitigation of radiation-induced damage. Additionally, high rates of glycolysis and critical changes in redox metabolism have been linked to GBM radioresistance and metabolic reprogramming, highlighting the intricate interplay between the tumor microenvironment and the radiation response (Marampon et al., 2014).

1.3.1 Contribution of Enhanced DNA Damage Response to Radioresistance in GBM

Radiotherapy stands as a cornerstone in cancer treatment, exerting its primary effect by inducing DNA damage within tumor cells. The efficacy of RT hinges on the induction of lesions in tumor DNA, initiating intricate biological responses collectively known as the DNA damage repair response (DDR). In the context of GBM cells, the DDR mechanism plays a pivotal role in their resistance to RT. DDR involves signal transduction pathways that coordinate cell cycle arrest and DNA repair, ultimately fostering cell survival (Biau et al., 2019).

DNA single-strand breaks are primarily repaired through the recruitment and ribosylation of PARP1, initiating the activation of effector DNA repair proteins. On the other hand, DNA double-strand breaks are predominantly repaired through non-homologous end joining (NHEJ) and homologous recombination (HR). HR is confined to the late-S/G2 phases of the cell cycle and is orchestrated by ATM and ATR. ATM is recruited to DSBs by the MRE11–RAD50–NBS1 (MRN) complex, a crucial step in initiating signal transduction in response to ionizing radiation. Both ATM and ATR contribute to the phosphorylation of the histone variant γ-H2AX, leading to CHK2, p53, and MDM phosphorylation and subsequently inducing G1/S arrest (Pilié et al., 2019). This intricate repair and signaling mechanisms underscore the elaborate cellular responses involved in maintaining genomic stability following radiation-induced DNA damage (**Figure 1.1**).

The ATM protein kinase, a key player in DDR, initiates downstream events crucial for coordinating cell cycle progression with DNA repair. Activated checkpoints, responding to DNA double-strand breaks, delay cell cycle progression to prevent the propagation of a mutated genome. The G2/M checkpoint specifically halts cell entry into mitosis until damaged or incompletely replicated DNA undergoes sufficient repair (Godinez et al., 2020). The cell cycle phase dictates the relative radiosensitivity of tumor cells, with cells being most

radiosensitive in the G2/M phase, less sensitive in the G1 phase, and the most resistant in the late S phase (Deckbar et al., 2011). Abnormalities in cell cycle checkpoints can regulate the radiosensitivity of GBM cells, providing insights for therapeutic strategies targeting this aspect of radioresistance (Li et al., 2022).

Resistance of GBM to RT is complex, involving factors like hypoxia hindering reactive oxygen species needed for cell elimination, a robust DNA damage response system, and ongoing communication among different tumor microenvironment populations through shared pathways. In radioresistant GBM cells, Wnt-induced signaling protein 1 (WISP1) plays a crucial role in cell survival, influencing immunosuppressive macrophage polarization through autocrine and paracrine signaling (Ren et al., 2023). The lysine methyltransferase enhancer of zeste homolog 2 (EZH2) is upregulated by radiation, stabilized by NIMA-related kinase 2 (NEK2) phosphorylation, and activated by maternal embryonic leucine-zipper kinase (MELK), ultimately methylating NF-κB to sustain glioma stem cell (GSC) transcriptional programs (Kim et al., 2015; Liu et al., 2019). Recent research indicates that radiation-induced senescent GBM cells promote the infiltration of Ly6G+ inflammatory, myeloid-derived cells, leading to the dedifferentiation of GBM cells into resistant GSC cells (Jeon et al., 2019; Ou et al., 2020).

The JAK/STAT pathway, a commonly altered pathway in various cancer types, exhibits heightened STAT3 activation in recurrent tumors and radioresistant GBM cells. However, only inhibiting STAT3 activity proves inadequate, as it activates ERK1/2, enabling GBM cells to survive radiotherapy (Gray et al., 2014). Furthermore, the transcription factor Forkhead Box Protein M1 (FOXM1) directly interacts with STAT3 in irradiated GBM cells, contributing to DNA damage repair, cell proliferation, and metastasis regulation. (Maachani et al., 2016) Inhibiting suppressors of cytokine signaling (SOCS) has been associated with increased radioresistance in glioma cells, with emphasis on the role of SOCS3 in GBM radioresistance. Methylation of the SOCS3 promoter may correlate with a poor prognosis in GBM patients (Ali et al., 2020). Inhibiting radiation-induced SOCS proteins in glioma cells may activate the JAK/STAT pathway, highlighting its significant role in GBM radioresistance.

In RT-resistant GBM cells, it has been observed that Smo is overexpressed, characterized by altered regulation in the DNA damage response. Smo is a component of the hedgehog pathway known for its anti-apoptotic, pro-proliferative, and pro-DNA repair functions. Knockdown of Smo in recurrent GBM cells previously exposed to radiation results in increased G2/M arrest and apoptosis. Furthermore, Smo upregulates ubiquitin-specific protease 3 (USP3) transcription, stabilizing claspin, which, in turn, binds to Chk1, facilitating its phosphorylation by ATR (Ou et al., 2020). In malignant gliomas, another factor identified as PDZ binding kinase, enriched and contributing to resistance, acts as a transcriptional activator of CCNB2 expression in a radiation dose-dependent manner. CCNB2 is an essential component of the cell cycle regulatory machinery (Ou et al., 2020).

1.4 Epigenetic Regulation and Glioblastoma

1.4.1 Epigenetics and Chromatin Modifiers

Epigenetic mechanisms regulate gene expression patterns through chemical modifications of DNA bases, histones, and changes to the chromosomal superstructure without affecting the DNA sequence. Eukaryotic DNA is packaged into chromatin by wrapping around a nucleosome that contain two copies of each core histone (H2A, H2B, H3, and H4). Accessibility of chromatin and the decision for a loosened (euchromatin) or a more tightly packed (heterochromatin) state, is regulated through histone modifications and DNA methylation.

Regulation of chromatin is controlled significantly through post-translational modifications (PTMs). These modifications can affect chromatin structure, gene function, and expression, and are involved in DNA repair and replication. Histone PTMs are dynamically added or deleted to certain residues by modifier enzymes. These enzymes are defined as writers that add PTMs to histones; erasers, which remove specific PTMs from histone substrates; and finally readers, which are proteins that recognize specific marks on histones. Reader proteins can also recognize a combination of marks and histone variants to direct a particular transcriptional outcome.

1.4.2 Histone Post-Translational Modifications and DNA Repair

Maintaining genome stability is crucial for cells exposed to numerous DNA damages, which can be affected by exogenous factors such as exposure to IR, UV, and environmental toxins, or endogenous factors such as reactive oxygen species or DNA replication errors. Depending on the type of genotoxic agent, this can result in various types of DNA lesions, including DNA base damage, SSBs, DNA inter-strand crosslinking, and DSBs. Cells have developed multiple efficient repair pathways to respond to these DNA damages. The most genotoxic DNA lesion on eukaryotes is DSB resulting in the breakage of both DNA strands (Karakaidos et al., 2020). Once DSBs are detected by the eukaryotic cellular machinery, two main pathways are used to maintain genome integrity, several alternative pathways can join DSBs, NHEJ which is the intrinsically error-prone pathway and HR which uses sister chromatid as a template therefore mainly active during the S and G2 phases of the cell cycle (Mao et al., 2008).

During DNA damage detection and repair, histones can undergo PTMs, including phosphorylation, acetylation, methylation, and ubiquitylation, to alleviate the physical constraints of the chromatin environment, mark the region as damaged, and serve as a mediator of the DDR signaling pathway and a platform for the assembly of effector proteins (Wei et al., 2018 & Gong et al. 2017). Among the histone PTMs, the lysine modification is reversibly controlled by histone acetyltransferases (Ali et al.,2020) and deacetylases (HDAC), respectively adding and removing of acetyl groups to lysine residues of histones H3 and H4. Methyltransferases catalyze the transfer of one, two, or three methyl groups to lysine or arginine residues of histone proteins (HKMTs for lysine and PRMTs for arginine). Histones are phosphorylated mainly on serine, threonine, and tyrosine by protein kinases and dephosphorylated by phosphatases (Biterge et al., 2016).

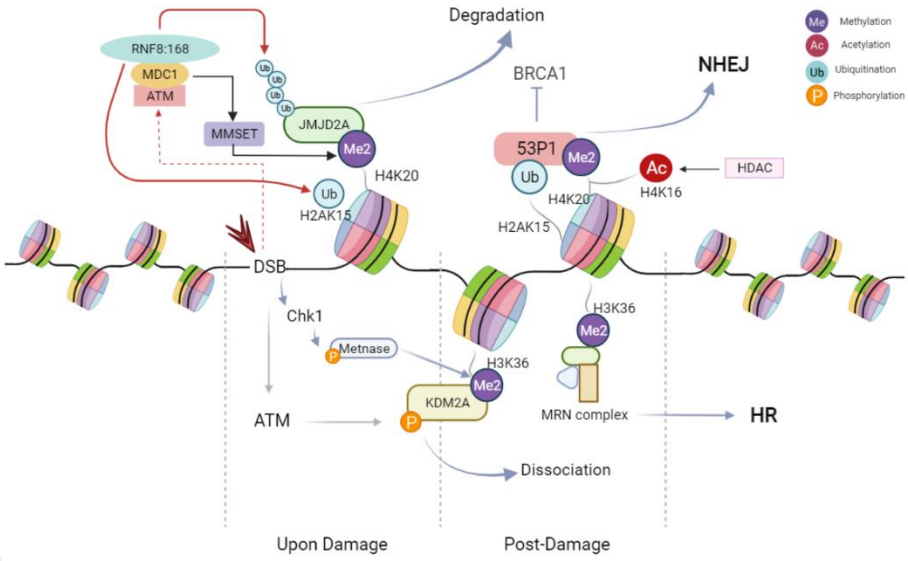

Figure 1.2 Different forms of post-translational modifications in various DNA repair pathways. Figure adapted from (Wei et al., 2018)

ATM-mediated phosphorylation of a histone demethylase, KDM2A, promotes its dissociation, which binds MRN complex to H3K36me2 and thus HR repair, from di-methylated H3K36. Besides, ATM-mediated recruitment of MDC1 and its interactions with other proteins provide bivalent recognition of 53P1, which prefers NHEJ as a final decision (**Figure 1.2**).

Histone phosphorylation

Phosphorylation of all histones has been reported to play a pivotal role in transcription, apoptosis, and mitotic chromosome condensation (Hanks et al., 1983). Regarding DNA damage response, H2A phosphorylation has been extensively studied. In the literature, the study about chromatin modification associated with DSB demonstrated that H2A phosphorylation, specifically the phosphorylated H2AX (γ-H2AX) occurs a few minutes after exposure to IR, and it is critically important to recruit signal/repair proteins to DNA damage sites (Rogakou et al., 1999). It was later shown that γ-H2AX may occur in all cell cycle phases and is required to activate checkpoint proteins during arrest (Stewart et al., 2003) and recruit DNA repair proteins in damage sites, thereby, involved in diverse DDR pathways. Studies on H2AX null mice have shown that γ-H2AX increases the efficiency of

DNA repair and reduces radiosensitivity, since the mice are highly radiosensitive, have abnormal genomes and also their DNA damage repair mechanism requires a longer time (Celeste et al., 2003). Upon DNA damage, the MRN complex and NBS1-mediated ATM, which promotes phosphorylation of adjacent histone H2AX, relocalizes to the break site. γ-H2AX facilitates the recruitment of DDR component DNA damage checkpoint protein 1 (MDC1). Rad51 is the critical protein that drives HR, and although it does not co-localize with MDC1, an overall decrease in nuclear Rad51 levels in response to IR has been observed in the absence of MDC1. Though MDC1 does not directly affect Rad51 assembly to DSBs, it can be suggested that the role of MDC1 in HR is mediated by regulation of Rad51 stability (Coster et al., 2010).

Histone acetylation

Histone acetylation, which has also been extensively studied in the context of both transcription and DNA damage repair, is dynamically regulated by a balance between HATs and HDACs (Grunstein et al., 1997). TIP60, MOF, GCN5, SW1/SNF, and p300/CBP are well-studied HATs involved in chromatin dynamics in the nucleus (Gong et al., 2013). As an example, histone H4, H2A, and H2AX are acetylated by NuA4-TIP60 complex at DSBs (Jacquet et al., 2016) thereby facilitating chromatin opening and improved DSB repair (Bird et al., 2002). In addition to chromatin relaxation, Tip60-dependent H4K16 acetylation reduces 53BP1 binding to H4K (Jacquet et al., 2016) and promotes HR repair (Tang et al., 2013). Histone H3 and H4 acetylation by CBP and p300 in conjunction with the SW1/SNF complex enhances the recruitment of NHEJ proteins as Ku70/80 (Ogiwara et al., 2011); and also activates transcriptionally BRCA1 and RAD51 genes, which are involved in HR repair (Tang et al., 2013). Furthermore, knockdown of p300 and ATP-dependent chromatin remodeler CHD4 has been shown to suppress the recruitment of replication protein A (RPA), an essential protein for HR repair, to DSB sites (Qi et al., 2016). Moreover, CBP and p300 depletion resulted in decreased RPA protein, which was followed by CHK1 phosphorylation and activation of the G2/M damage checkpoint, indicating that CBP and p300 play several roles in the activation of the cellular response to DSBs (Ogiwara et al., 2011).

Histone methylation

Histone methylation is crucial for proper genome programming and has been best studied for its roles in transcriptional regulation and DNA damage response. Unlike acetylation, methylation does not alter the charge of arginine and lysine residues, but alters the interactions required for chromatin restructuring. The identification of histone demethylases in the literature has shown that methylation is reversible and justifies their function in DSB repair (Hunt et al., 2013). For example, a study of the histone demethylase KDM5A as a key regulator of the bromodomain protein complex showed that KDM5A-dependent H3K4me3 demethylation is observed in chromatin near DSB sites (Gong et al., 2017). Moreover, their findings show that the repair mechanism of DSBs by HR is impaired in the case of KDM5A deficiency.

The histone methylation with different combinations operates as an insertion site for various effector proteins involved in the HR or NHEJ pathway, which may influence the ultimate decision (Wei et al., 2018). For instance, different forms of methylated H3K36 play dual roles in DNA repair pathway selection depending on the total number of methyl groups added and the cell cycle phase (Fnu et al., 2011). The requirement of SETD2-dependent tri-methylated H3K36 for HR repair and maintenance of genome stability has been demonstrated in several studies. Interestingly, H3K36me3 does not occur with DNA damage, it already exists, but SETD2-mediated H3K36me3 provides binding sites for LEDGF (Gong et al., 2013) via the PWWP domain therefore it is masked. After DSBs, LEDGF promotes the recruitment of CtIP resulting in resection and facilitating recruitment of RPA and RAD51 which are HR-related proteins (Daugaard et al., 2012). In the absence of SETD2, a tumor suppressor, it has been shown that the decrease in H3K36me3-mediated HR repair observed in cancers such as breast, renal, prostate, and lung results in impaired mismatch repair and genome stability (Xiao et al., 2021). Besides, di-methylated H3K36 functions in post-damage of DNA, catalyzed by METNASE phosphorylated by Chk1, and promoting its uptake into DSBs (Wei et al., 2018). However, H3K36me2 is masked to impair its performance by its specific demethylase (KDM). Interestingly, while DNA damage has been shown to induce degradation of KDM2A and KDM4A, ATM mediates the phosphorylation of KDM2A for its dissociation from H3K36me, however, that results in the recruitment of the MRN complex

to induce DNA repair. Additionally, DSBs trigger RNF8- and RNF168-mediated degradation of KDM4A, although DDR can compensate for degradation by inhibiting the activity of H3K36 methylation, which encourages another pathway in DDR. As such, this reduction in KDM4A allows exposure of H4K20me2 to facilitate the uptake 53BP1 into DSBs (Gong et al., 2017).

The methylation of H4K20 increases locally upon the induction of DSBs (Pei et al., 2011) which may favor providing docking sites for the DDR factor 53BP1 (Gong et al., 2017) that plays as a bivalent reader of histone modifications, promotes checkpoint signaling and switches the pathway choice to NHEJ or HR (Gong et al., 2017). Upon DSBs, ATM facilitates the recruitment of MDC1 to accumulate at DSBs, following RNF8/RNF168, which modify masking proteins of H4K20me2 (L3MBTL1, JMJD2A) as illustrated in **Figure 1**.**2**. In another related study, loss of RNF168 has been concluded to impair the binding of 53BP1 at bivalent recognition of both H2A/H2AXK15ub and H4K20me2. Ubiquitylated L3MBTL1 and JMJD2A are degraded or disassociated from H4K20me2 via MDC1-mediated MMSET. That provides accessibility of 53BP1 to demethylated H4K20 (Gong et al., 2017). Tri-methylated H3K9, linked to the DNA damage response, plays a role in initiating a homologous recombination (HR) pathway by facilitating chromatin opening and the recruitment of repair proteins. Following DNA double-strand breaks (DSBs), the interaction between Tip60 and H3K9me3 becomes crucial. This interaction activates Tip60's acetyltransferase activity, ensuring the recruitment of the MRN complex. The MRN complex is pivotal for the repair process. This process underscores the intricate role of histone methylation in regulating DNA repair pathways, showcasing the dynamic and precise cellular response to DNA damage. (Kaidi et al., 2013).

Specific interactions between histone modifications and proteins involved in cellular metabolism play a critical role in generating the damage identification signal and governing epigenetic information that determines repair pathway choice. The DNA damage response triggers a transduction pathway that seizes control of the cell cycle, restricting the mitotic entry of cells containing DNA lesions and thereby blocking cells at G2/M.

As part of a complementary initiative at our Koç University Brain Cancer Research Laboratory, a chemical screen was conducted using a library of 146 epigenetic regulatory

proteins. This screen, incorporating low doses of the chemical library in conjunction with a 4 Gy treatment, aimed to identify epigenetic regulators that could enhance the response to RT. Given that ionizing radiation induces damage intricately linked with the DNA damage response, this approach offered a comprehensive assessment. Remarkably, among the selected 'hit drugs' emerging from the screen were inhibitors targeting protein arginine methyltransferases (**Figure 1.2**). The identification of PRMT inhibitors as potential radiosensitizers is particularly promising, considering the dual role of PRMTs as not only epigenetic modifiers but also integral components in DNA damage response and repair pathways. This finding positions PRMTs as promising and multifaceted targets for advancing radiosensitization strategies.

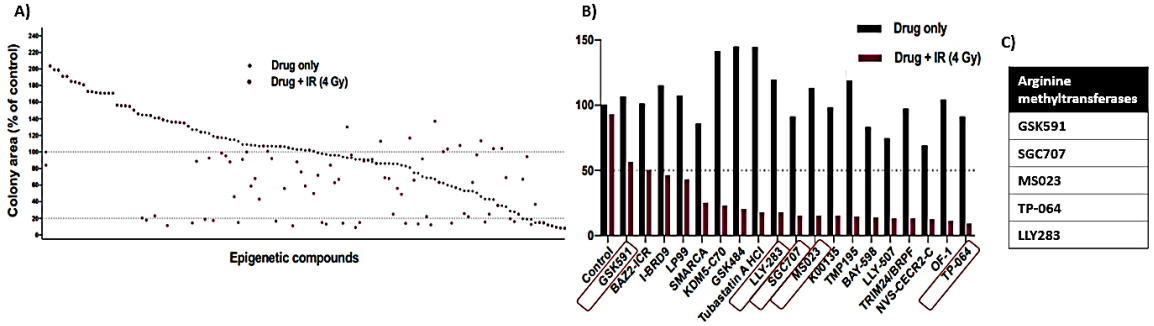

Figure 1.3 Epigenetic chemical screen results. **A)** Clonogenic cell viability test after drug screening. **B)** Chemicals determined to be significantly affected by the combination of drugs and radiation on cell viability. **C)** Arginine methyltransferase drugs determined to be effective. Screen was performed by Nareg Pınarbası-Degirmenci as part of her thesis.

1.4.3 Protein arginine methyltransferases (PRMTs)

Post-translational modification involves chemically altering proteins by adding chemical groups and diversifying their functions. Protein arginine methylation is a versatile post-translational modification observed in both histones and nonhistone proteins. PRMTs act as "writers" in this process, influencing transcription, pre-mRNA splicing, and DNA damage responses. Arginine methylation, a lesser-studied modification compared to acetylation or phosphorylation, has gained recent attention in the context of cancer due to challenges in substrate detection and developing selective inhibitors. PRMT inhibitors, targeting this

modifiable process, show promise as cancer therapies, with potential benefits observed in preclinical and clinical settings (Hwang et al., 2021).

PRMTs are classified into three distinct types based on their specific enzymatic activities. Type I PRMTs (including PRMT1, 2, 3, 4, 6, and 8) catalyze the formation of asymmetric dimethylarginine (ADMA) residues on target proteins, while Type II PRMTs (PRMT5 and 9) facilitate the creation of symmetric dimethylarginine (SDMA) residues. On the other hand, Type III PRMTs (PRMT 7) are responsible for the addition of monomethyl arginine residues to target proteins (Yang et al., 2013). These enzymes play pivotal roles in various cellular processes, such as gene expression regulation, RNA processing, signal transduction, and the modulation of protein-protein interactions (Yang et al., 2013). Dysregulation of arginine methylation, mediated by PRMTs, can have profound implications for cellular function and is implicated in the pathogenesis of diseases, including cancer and neurological disorders. Consequently, understanding the classification and function of PRMTs is essential for advancing research in these fields and exploring potential therapeutic interventions.

Hwang et al. (2021) comprehensively reviewed the relationship between PRMT and cancer, along with current therapeutic approaches. According to this review, PRMTs constitute a vital family of enzymes implicated in cancer biology through post-translational modifications. The diverse roles of PRMTs in cancer span both tumor-suppressive and tumor-promoting functions, with their dysregulation often observed in various malignancies. For instance, PRMT1 has been linked to aberrant apoptosis, cell cycle progression, and DNA repair mechanisms in cancer cells. Another member, PRMT2, serves as a potential target for cancer therapy due to its involvement in oncogenic gene expression and apoptosis. PRMT4 (CARM1) influences cancer by participating in super-enhancer–mediated transcription and collaborating with BRD4 and PARP1 in crucial cellular processes. PRMT5, often upregulated in cancer, regulates gene expression, including oncogenes and tumor suppressors. Moreover, PRMT6, associated with GBM, plays a role in mitotic activity, nucleocytoplasmic transport, and cell proliferation. The clinical implications of PRMT dysregulation extend to potential biomarkers for certain cancers and the development of therapeutic strategies, including the exploration of small molecule inhibitors targeting PRMT activity.

The literature on the role of PRMT inhibitors in cancer suggests that they may influence fundamental cellular processes such as cell cycle regulation, DNA repair, and proliferation. Although the expressions and roles of PRMT class enzymes have been recently identified in different cancer types, their effects on radiotherapy in GBM remain unknown. While expressions and roles of PRMT class enzymes have been recently identified in different cancer types, their effects on radiotherapy in GBM are yet to be elucidated. Our findings, in accordance with these suggestions, support the notion that PRMT inhibitors can induce significant effects on GBM cells. The alignment with existing literature enhances the validity and importance of our study.

In this thesis, we investigate various drugs designed to target specific members of the PRMT enzyme family. SGC707 targets to inhibits on PRMT3, and LLY283 selectively inhibits PRMT5. MS023 is designed for Type-I PRMTs, including PRMT1, PRMT3, PRMT6 and PRMT8. Also, MS049 targets PRMT4 (CARM1) and PRMT6. These investigations provide insights into the potential therapeutic applications of these drugs within the intricate context of PRMT inhibition in cancer treatment.

1.4.4 Role of Epigenetic Modifications in GBM Progression and Therapy Response

Cancer progression is not only driven by genomic alterations but is profoundly influenced by epigenetic modifications, encompassing the activation of oncogenes and repression of tumor suppressor genes. The dynamic "epigenomic landscape" of tumor cells undergoes significant alterations during oncogenesis and in response to therapeutic interventions (Brien et al., 2016). Glioblastoma, among various cancers, exhibits distinct epigenomic variations that contribute to sustained cell survival and the acquisition of therapy resistance. Global genomic hypomethylation, a characteristic feature of GBM, contributes to genomic instability and the activation of proto-oncogenes . The methylation status of the MGMT promoter, a recognized predictive biomarker, is closely linked to the response of GBMs to TMZ. Within GBM, epigenetic modifications involve the methylation of lysine and arginine residues on histone H3 and H4, with frequent alterations observed at H3K4, H3K9, H3K27, and H3K36 (Rivera et al., 2019).The upregulation of EZH2 and the identification of the H3K27M mutation in a subgroup of pediatric gliomas highlight the intricate interplay between epigenetic modifications and GBM pathogenesis. The Polycomb Repressive Complex 2 (PRC2)

complex, under the regulation of lysine demethylases KDM6A and KDM6B, plays a crucial role in these processes, impacting therapy response in both preclinical and clinical trials (Laugesen et al., 2016). Additionally, the disruptions caused by isocitrate dehydrogenase 1/2 mutations in primary glioblastomas and WHO grade II astrocytomas, leading to the accumulation of the oncometabolite D-2-hydroxyglutarate (D2HG), underscore the critical role of metabolism in epigenetic regulation (Huang et al., 2019). HDAC also play a significant role, with high expression contributing to changes in the transcriptomic profile, enabling evasion of cell death.

In this thesis, we have delved into the examination of the combined effects of PRMT inhibition and radiation on glioblastoma cells. Our focus has been on unraveling the intricate interplay between PRMTs, crucial epigenetic regulators, and the cellular response to radiation. By investigating the impact of PRMT inhibition on radiosensitivity, we aim to contribute valuable insights to the field, potentially paving the way for novel therapeutic strategies in the management of GBM. Through our exploration of these interactions, we seek to advance the understanding of the underlying mechanisms influencing GBM cell response to radiation.

Chapter 2:**MATERIALS AND METHODS**

2.1 Cell culture

Glioblastoma cell lines U373 and U87MG were purchased from American Tissue Type Culture Collection (USA) and were maintained in DMEM, supplemented with 10% FBS (Gibco, USA) and 1% Penicillin-Streptomycin (Gibco, USA), at 37°C in a humidified incubator with 5% CO2 incubator. Cells were grown in 10 cm petri dishes or T75 flask and were routinely checked for mycoplasma contamination by Lonza Mycoplasma Detection Kit.

2.2 Cell viability and proliferation assays

2.2.1 Cell Titer Glo Assay

Cell viability was determined via Cell Titer-Glo® (CTG) Luminescent Cell Viability Assay (Promega, USA). The CTG assay determines the number of viable cells in the culture through the luciferase reaction based on the determination of the amount of ATP, an indicator of metabolically active cells. CTG assay was slightly modified from the manufacturer's instructions.

For CTG, 1 x 10^3 cells per well were seeded in triplicates into black 96 well plates for each condition. In accordance with the experimental plan, at an appropriate time in drug and/or radiation treatment, each plate was incubated for 5 minutes at room temperature before CTG reagent addition. For 96 well plates, medium was removed and 4 µl CTG reagent + 40 µl of DMEM mix was added per well for attached cells. For spheres, 7 µl CTG was directly added to the well without DMEM removing step. Then, the plate was put into Synergy H1 Reader (Biotek, USA) for 2 minutes of shaking and 8 minutes of incubation at dark before the luminometric read. Survival was quantified by determining the percentage of viable cells within the treated sample in relation to the untreated control samples.

2.2.2 Clonogenic Assay

Clonogenic assay investigated a cell's survival, proliferation, and colony formation capacity. 750 cells/well were seeded in triplicate into 6-well cell culture plates. The next day, PRMT

inhibitors were administered and incubated for a duration ranging between 24 to 72 hours according to the experimental plan. After drug incubation, each plate was exposed to a single dose of 2 Gy or 4 Gy ionising radiation. After incubating cells for 10–14 days, wells were washed twice with 1x DPBS, and colonies were fixed with ice-cold methanol treatment for 10 min. After fixation, the wells were washed twice with 1x DPBS and incubated with crystal violet for 30 min with gentle shaking. Colony quantifications were performed by Image J analysis using the ColonyArea plugin.

Figure 2.1 Experimental approach for functional validation of screen results

2.3 Chemical inhibitors

PRMT inhibitor compounds LLY283, SGC707, MS023, and MS049 were purchased from SelleckChem and their main stocks were dissolved with DMSO to 10 mM. Then, it was diluted to 1 mM with DMSO and aliquoted.

Compounds	Target	Working Con.
LLY283	Arginine methyltransferase - PRMT5	0.5 µM
SGC707	Arginine methyltransferase - PRMT3	2 µM
MS023	Arginine methyltransferase - Type I PRMTs	2 µM
MS049	Arginine methyltransferase – PRMT4, PRMT6	2 µM

Table 1. PRMT inhibitors and their working concentrations

2.3.1 IC50 determination/dose response calculation

To calculate IC50, 2 x 10^3 cells were seeded in a 96-well black plate and treated with a series of dose drugs the next day. Then, cell viability analyzed with CTG.

2.4 pH2A.X assay

The Muse H2A.X Activation Dual Detection Kit (Cat. MCH200101) was used to evaluate DDR activation following slightly modified supplier's instructions. The assay consists of directly conjugated antibodies: anti-phospho-histone H2A.X (Ser139) - Alexa Fluor®555 and a phospho-specific histone H2A.X PECy5-conjugated antibody to measure activation of the H2A.X. This kit is designed to simultaneously detect the phosphorylation status of Histone H2AX by flow cytometry analysis. 500.000 cells/well were seeded into 6-we culture plates. The next day, PRMT inhibitors were administered and incubated for 48 hours. After drug incubation, cells were exposed to a 4 Gy ionising radiation dose. Then, the cells were collected at certain intervals, centrifuged at 300 x g for 5 min and washed with 1X PBS. The harvested cells were centrifuged at 300 x g for 5 min, and the supernatant was discarded. A 1 mL volume of a 1: 1 mixture of assay buffer (1×) and the fixative solution was added to the cell button to be carefully suspended and allowed to stand for 5 min on ice. Subsequently, the cells were centrifuged at 300 x g for 5 min, and the supernatant was discarded. Cells were permeabilized with 500 µL of permeabilization buffer for 5 min on ice. At the end of this period, the cells were centrifuged at 300 x g for 5 min, and the supernatant was discarded. To the cell button, 95 µL of assay buffer (1X) and 5 µL of a 1:1 solution of antibodies were added, and it was incubated for 30 min at room temperature, in the dark. 100 µL of 1x assay buffer was added to the cells, centrifuged at 300 x g for 5 min, and the supernatant was discarded. Finally, the stained cells were suspended in 200 µL of assay buffer to be later quantified using the Muse® Cell Analyzer Cat No. 6500-3115 cytometer. Data generated by the Muse® Cell Analyzer and the corresponding Muse software module provide statistical values measuring the percentage of H2AX-activated cells.

2.5 Gene expression analysis by qRT-PCR

To determine respective mRNA expression, U373 cell pellets were collected and RNA isolation was performed with NucleoSpin® RNA Isolation Kit according to manufacturer's instructions (Macherey-Nagel). RNA concentrations were measured with Nanodrop. With reverse transcriptase reaction, 1000 ng of cDNA was obtained by using M-MLV Reverse Transcriptase (Invitrogen). mRNA expression levels of certain genes were detected by

LightCycler® 480 SYBR Green I Master (Roche). Sequences of used primers are listed in Table 1.

2.6 CRISPR/Cas9 plasmid cloning

Genes indicated in **Table 1** targeting gRNAs were cloned into plentiGuide-puro backbone according to ZhangLab's protocol (Ran et al., 2013). In summary as illustrated in **Figure 2.6**, the plentiGuide-puro vector was digested with BsmBI Restriction Enzyme and gel purified with MN PCR-Clean Up Kit. 1 µl of each oligo (100 µM) was annealed with T4 Polynucleotide Kinase and T4 DNA Ligase Buffer in 10 µl reaction in a thermal cycler with the following settings: 37°C for 30 min, 95°C for 4 min and then ramp down to 25°C at 5°C/min. The annealed oligos (**Table 2)** were diluted 1:200 and used as inserts. Then, each one µl of inserts was ligated with 50 ng BsmBI-digested vectors using T4 DNA Ligase (NEB) in 10X T4 DNA Ligase buffer (NEB). The ligation reaction occurred at 16°C overnight.

Afterwards, the transformation was applied using 50 µl Stbl3 bacteria mixed with 5 µl of the ligation reaction for 15 minutes on ice following heat shock at 42°C for 45 seconds. Later, 300 µl Luria-Bertani (LB) broth was added and cultured in 37°C at 225 rpm in a shaker for an hour. The reaction was spread on Carbenicillin resistant plates and incubated overnight at 37°C. Next day colonies were picked individually, grown in LB and plasmid DNA was extracted by MN Nucleospin Plasmid Kit. To confirm the inserts, samples were sent to sequencing to Macrogen Europe with U6 promoter sequencing (Forward sequencing primer for U6 promoter ACTATCATATGCTTACCGTAAC).

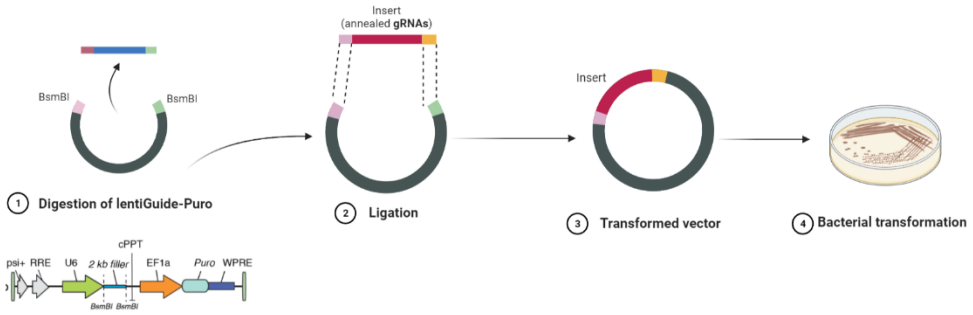

Figure 2.6 Experimental approach for selected gRNAs that were cloned into the plentiGuide-puro vector.

Table 2. Sequences of oligonucleotides used for gRNA cloning

	FORWARD	REVERSE COMPLEMENT
G_PRMT1-1	CACCGCTCACCGTGGTCTAACTTGT	AACACAAGTTAGACCACGGTGAGC
G_PRMT1-2	CACCGGGATGTCATGTCCTCAGCGT	AACACGCTGAGGACATGACATCCC
G_PRMT1-3	CACCGTTTGACTCCTACGCACACTT	AACAAGTGTGCGTAGGAGTCAAAC
G_PRMT3-1	CACCGGCCATGTGCTCGTTAGCGTC	AACGACGCTAACGAGCACATGGCC
G_PRMT3-2	CACCGGCCTGACGCTAACGAGCACA	AACTGTGCTCGTTAGCGTCAGGCC
G_PRMT3-3	CACCGGAATTCATGTACTCAACTGT	AACACAGTTGAGTACATGAATTCC
G_PRMT5-1	CACCGCGGAATGCGGGGTCCGAACT	AACAGTTCGGACCCCGCATTCCGC
G_PRMT5-2	CACCGCAGCATACAGCTTTATCCGC	AACGCGGATAAAGCTGTATGCTGC
G_PRMT5-3	CACCGATGAACTCCCTCTTGAAACG	AACCGTTTCAAGAGGGAGTTCATC
G_PRMT6-1	CACCGTCCTCCACGCGCGAACCAAG	AACCTTGGTTCGCGCGTGGAGGAC
G_PRMT6-2	CACCGGCCCATCCACTCGCTCACGA	AACTCGTGAGCGAGTGGATGGGCC
G_PRMT6-3	CACCGCCTCTACCGCGTACACGCGC	AACGCGCGTGTACGCGGTAGAGGC
G_PRMT8-1	CACCGGTCGAAGTAATAATCTCTCG	AACCGAGAGATTATTACTTCGACC
G_PRMT8-2	CACCGAGGTGCGGACTCTCACTTAC	AACGTAAGTGAGAGTCCGCACCTC
G_PRMT8-3	CACCGCCCTGCCTTGGCAGCGAACA	AACTGTTCGCTGCCAAGGCAGGGC

2.7 Lentiviral Packaging and Transduction

Initially, 2x10^5 HEK293T cells per well in a 6-well plate were seeded for the lentiviral packaging procedure. The next day, 50 ng of VSV-G (Addgene 8454), 450 ng of psPAX2 (Addgene 12260), and 500 ng of the target plasmid were combined and prepared in 40 µl serum-free DMEM **(Figure 2.7).** After that, this DNA combination was added to another 40 µl serum-free DMEM that had 4 µl of Fugene 6 (Roche Applied Science) in it. Carefully, 80 µl drops of the DNA-Fugene mixture were placed onto 6 cm plates. The media was changed following a 16-hour incubation period. For the control group, the plentiGuide_NT1 plasmid was packaged into viral particles for non-targeting (NT1). The viral particle-containing supernatant was collected 48 and 72 hours after transfection, and then it was filtered via 45-µm filters. The viruses were either directly aliquoted and viruses were then stored at -80°C until needed. For the determination of viral titers, 2x10^5 cells per well in a 6-well plate were transduced with 10, 1, 10-1, 10-2 µl of virus in the presence of 8 µg/ml protamine sulfate.

After a 16-hour incubation, the media was replaced. The following day, cells from each well were transferred to 10 cm plates in the presence of puromycin. Upon completion of puromycin selection for uninfected cells, transduced cells were counted and compared to uninfected/unselected parental controls. The viral volume corresponding to 30-50% transduction efficiency was considered as the Multiplicity of Infection (MOI) of approximately 0.3-0.4.

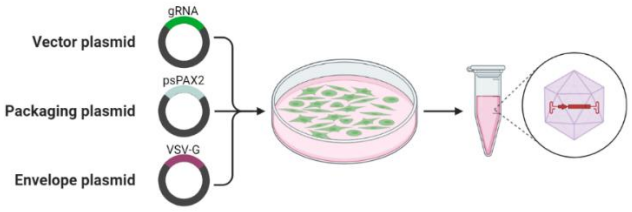

Figure 2.7 Experimental Approach for Plasmid Packaging in HEK 293T Cells

2.8 Establishing cell lines with PRMT knock out

Cas9-expressing stable cell lines were established in U373 by transducing cells with the LentiCas9-blast virus (Addgene #52962) at an MOI of 1. Following this, a selection process using blasticidin was carried out for 7 days. The verification of Cas9 expression was performed through qPCR analysis at the mRNA level.

PRMT knockout cell lines were established in U373-Cas9 stable by transducing cells with the construct cloned into the LentiGuide-Puro backbone (Addgene #52963). As illustrated in **Figure 2.8**, a selection process was conducted using 2 µg/ml puromycin for 3 days. The verification of knockout cell lines was performed through qPCR analysis at the mRNA level five days post-transduction. The qRT-PCR primer sequences are provided in **Table 3.**

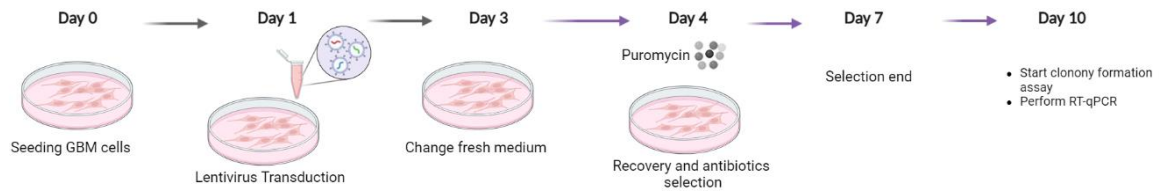

Figure 2.8 Transduction Procedure for Plasmid Packaging in U373-Cas9 stable cell line.

	FORWARD	REVERSE
PRMT1	TCGAGTGTTCCATCCTCTGC	TCCCCTTGATGATGGTCACC
PRMT3	GCATGGTTCATAAACATGGACTT	CACCCAACATCCAAAACTACC
PRMT5	CAGCAGGCCTCTCAGACATA	CTCCCAGCACCATCAGTACC
PRMT6	CGTTTCAGGAGAGATCACGC	TCTCCCACTCAGTCCTCCAT
PRMT8	CCTGGCACTTTGAGGTGTTG	GTCTGATGGAATGGGCCTG
GAPDH	CTCCTGCACCACCAACTG CT	GGG CCATCCACAGTCTTCTG

Table 3. qRT-PCR primer sequences

2.9 RNA Sequencing and Analysis

U373 cells were sequenced under four different conditions in triplicate. Control cells did not undergo drug or radiation treatment. MS023 was administered to the second group, the third group received 4 Gy IR, and the fourth group was subjected to both drug and IR treatments. Total RNA isolation was done via MN Nucleospin RNA isolation kit (Macherey Nagel, Germany). Library preparation and sequencing were performed at BGI Genomics (Hong Kong, China). The outputs generated from different lanes were consolidated before analysis. MultiQC analysis was employed for quality control assessment. The obtained paired-end fastq files underwent alignment to the reference human transcriptome (GRCh38) using the STAR algorithm. The SALMON algorithm, relying on Transcripts per Million (TPM), was utilized for transcript quantification. The DeSeq2 algorithm was employed for the identification of differentially expressed genes.

The lists of differentially expressed genes (DEGs) obtained were used as input for Gene Set Enrichment Analysis (GSEA). The GSEA software was applied with a default rank-ordered algorithm, utilizing all currently available gene sets (Subramanian et al., 2007).

2.10 Western Blotting

For whole cell extracts, cell pellets were lysed in an appropriate volume of lysis buffer including 1% NP-40, 150 mM NaCl, 1mM EDTA, 50 mM Tris-HCl (pH 7.8), 1 mM NaF,

0.1 mM PMSF, 1X phosphatase inhibitor cocktail (PhosSTOP, Roche) and 1X protease inhibitor cocktail (cOmplete Protease Inhibitor Cocktail Tablets, Roche). During 30 minutes of incubation on ice, the sample was vortexed every 10 minutes. At the end of the incubation, centrifugation was performed at 14,000 g for 15 minutes at 4ºC to obtain supernatants containing the total cell extract.

For nuclear fractionation, cell pellets were first resuspended in cytosolic lysis buffer 20 mM 7.9 pH HEPES, 10 mM KCl, 0.4% NP40, 0.1 mM EDTA and 1x Protease Inhibitor and 1x Phosphatase Inhibitor), incubated on ice for 15 minutes, and then centrifuged to collect the cytosolic fraction at 3000xg for 3 minutes. The remaining pellet underwent additional washing and was subsequently resuspended in nuclear buffer (10 mM 7.9 pH HEPES, 0.4 M NaCl, 10% Glycerol, 1 mM EDTA and 1x Protease Inhibitor and 1x Phosphatase Inhibitor) after sonication on ice (2x10 sec, amplitude 40). The resulting supernatant represented the nuclear fraction and was stored at -80°C.

To assess protein concentrations, the Pierce BCA Protein Assay Kit (Thermo Scientific, 23225, USA) was performed following the manufacturer's guidelines. For each sample, 50 µg of protein was utilized by combining 4X Laemmli buffer (Bio-Rad, 1610747, USA) and 10% beta-mercaptoethanol, with subsequent denaturation at 95°C for 5 minutes. The samples run on electrophoresis on a 4-12% Mini Protean TGX Precast Gel (Bio-Rad, 456-1044, USA). Protein samples were then transferred to a PVDF membrane using Trans-Blot Transfer System (Bio-Rad, USA) for 90 minutes at 100V. Following a 1-hour block at room temperature using 5% Bovine Serum Albumin in TBS-T, the membrane was subjected to overnight incubation with primary antibodies at 4°C. After three washes with 1X TBS-T at 15-minute intervals, the membranes were exposed to appropriate secondary HRP-conjugated antibodies (with a 1:5000 dilution) prepared in 5% non-fat dry milk. Membrane imaging was achieved using the SuperSignalTM West Femto Maximum Sensitivity Substrate (Thermo Scientific, 34095, USA) in the ChemiDoc XRS+ System (Biorad, USA).

Table 4. Primary antibody list utilized in western blotting

Antibody	Brand/Catalog Nu.	Dilution Rate	Dilution Solution
Anti- Histone H3 (D1H2) Antibody	Cell Signaling/ 4499	1:5000	TBS-T
GAPDH	Abcam/ab9485	1:5000	TBS-T
Symmetric Di-Methyl Arginine Motif	Cell Signaling/ 13222	1:2000	%5 BSA in TBS-T
Asymmetric Di-Methyl Arginine Motif	Cell Signaling/ 13522	1:2000	%5 BSA in TBS-T

2.11 Statistical Analysis

All normalizations were performed on the control group, which are non-radiated and untreated cells, denoted as 100%, using GraphPad Prism version 10.0 and Microsoft Excel Office 2016. Student's t-test or ANOVA determined significance with a p-value <0.05.

Chapter 3:**RESULTS**

3.1 Effects of ionizing radiation on the viability and proliferative behaviour of the human glioblastoma cells

To establish a standardized RT application regimen on GBM cells, we selected a cell line, U373 and tested its response to varying doses of irradiation. The U373 cells were irradiated with doses of 2, 4, 6, and 8 Gy as a single fraction treatment. Subsequently, we assessed both colony formation capabilities within these cell populations, as illustrated in **Figure 3.1**. Analysis of colonies, stained with crystal violet after a 14-day culture period, demonstrated a diminution in colony sizes among cells exposed to higher radiation doses. According to these findings, we selected 2-4 Gy irradiation as an optimal radiation dose for subsequent experiments.

A)

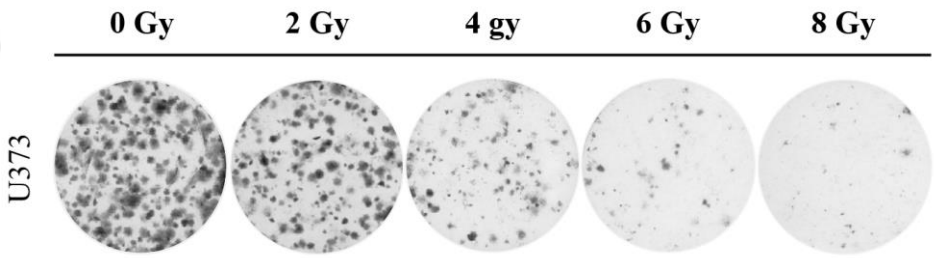

B)

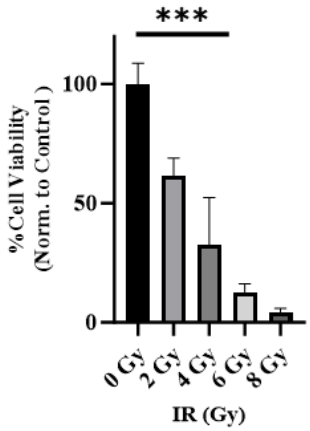

Figure 3.1: Effect of irradiation with a 2, 4, 6 and 8 Gy dose on the viability of U373 cell line. **A)** Representative colony formation assay of U373 treated with IR. **B)** Quantitative analysis of colony formation. (n=3), *** p< 0.001

3.2 Effects of different PRMTi on the viability and proliferative behaviour of human glioblastoma cells

As PRMT inhibitors were identified as potential radiosensitizers in our previous work, we aimed to elaborate on this finding with additional experiments. First, we tested the effects of the selected inhibitors (MS023, MS049, LLY283 and SGC707) on GBM cell viability as single treatments. We employed 3 GBM cell lines, U373, U87MG as established cells and GBM4 as a primary cell line. IC50 values for each drug were calculated for U373 cells **(Figure 3.2.1).** All GBM cell lines were similarly sensitive to the LLY283, but not to MS023, as GBM4 cells were not as much affected **(Figure 3.2.1 B)**.

A)

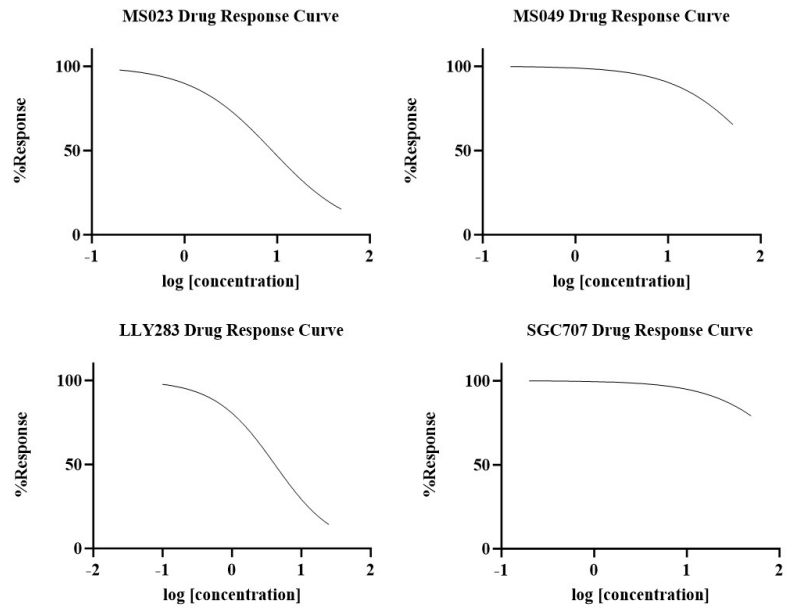

95% CI (profile likelihood)	*SGC707*	*LLY283*	*MS049*	*MS023*
LogIC50	0.7843	0.8569	1.051	0.8849
IC50	6.085	7.193	11.24	7.672

B)

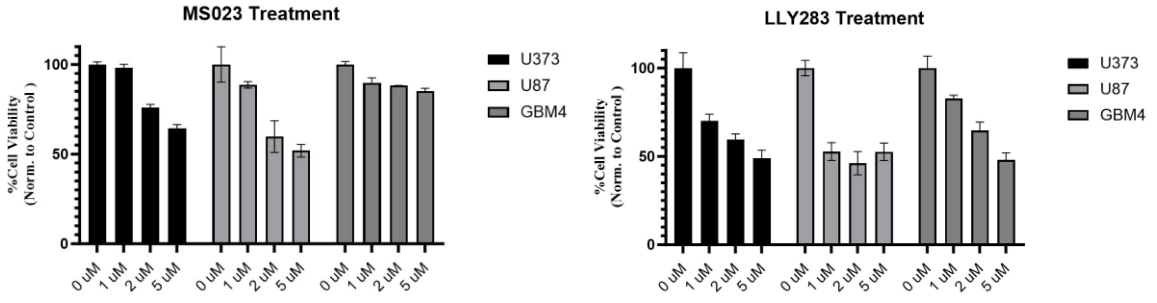

Figure 3.2.1 Effects of PRMT inhibitors on GBM cell viability. **A)** Dose-response curve and calculated IC 50 for effects on cell viability of U373 cells treated with PRMTs inhibitor drugs. **B)** Cell viability of U373, U87MG and GBM4 cells treated with MS023 and LLY283 by using CTG assay on 3rd day of drug incubation.

While CTG assay provides knowledge on cell growth, it may not be the best suited assay to test long term effects of treatments, as cells undergo contact inhibition due to overgrowth in a short time. Therefore, we conducted a clonogenic cell viability assay concurrently. The U373 cells were treated with 2 mM MS023, 2 mM MS049, 2 mM SGC707, and 0.5 mM LLY283 for 48 hours. Following this treatment, a medium change was carried out, and after 14 days, staining was performed using crystal violet (**Figure 3.2.2**). The results indicated a significant reduction of nearly 50% in the colony-forming capacity with the MS023 drug. However, no significant changes were observed with SGC707.

A)

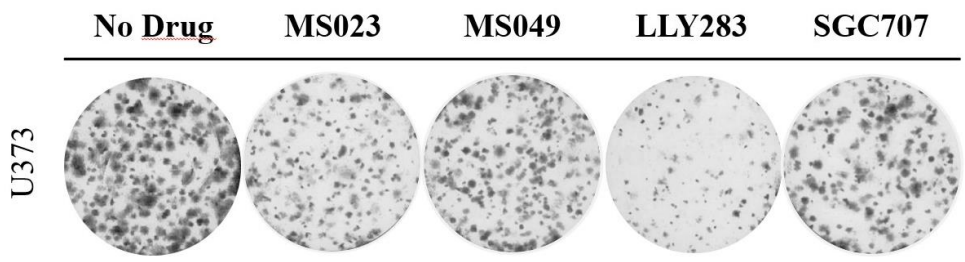

B)

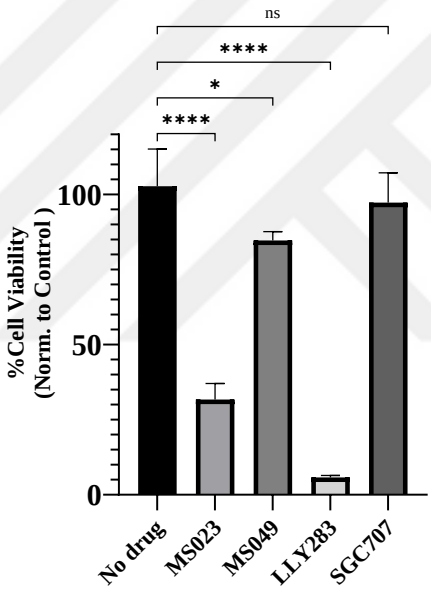

Figure 3.2.2. Effect of PRMT inhibitors on GBM cell colony formation. **A)** Representative colony formation assay pictures of U373 treated with different PRMT inhibitors. **B)** Quantitative analysis of colony formation. (n=3) * $p < 0.05$, **** $p < 0.0001$

3.3 Combining IR Treatment with Inhibition of PRMT Activity Reduces Viability, Proliferation, and Clonogenicity in U373 Cells

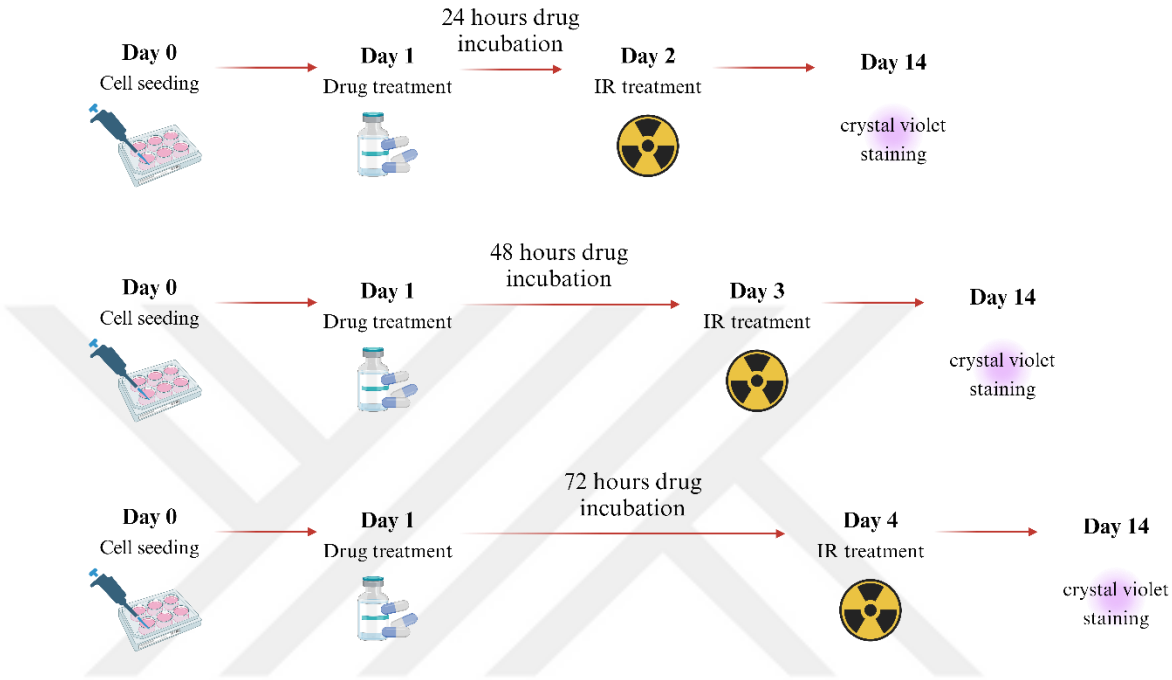

Figure 3.3 Experimental schema for the optimization of the period of drug treatment and IR.

3.3.1 Testing the effect of 24 h pre-treatment

To investigate whether selected drugs result in changes in long-term cell viability when combined with radiation, U373 GBM cells were treated for 24 hours and then received 2 and 4 Gy radiation. Colony-forming ability was measured after 14 days as illustrated in **Figure 3.3.1**.

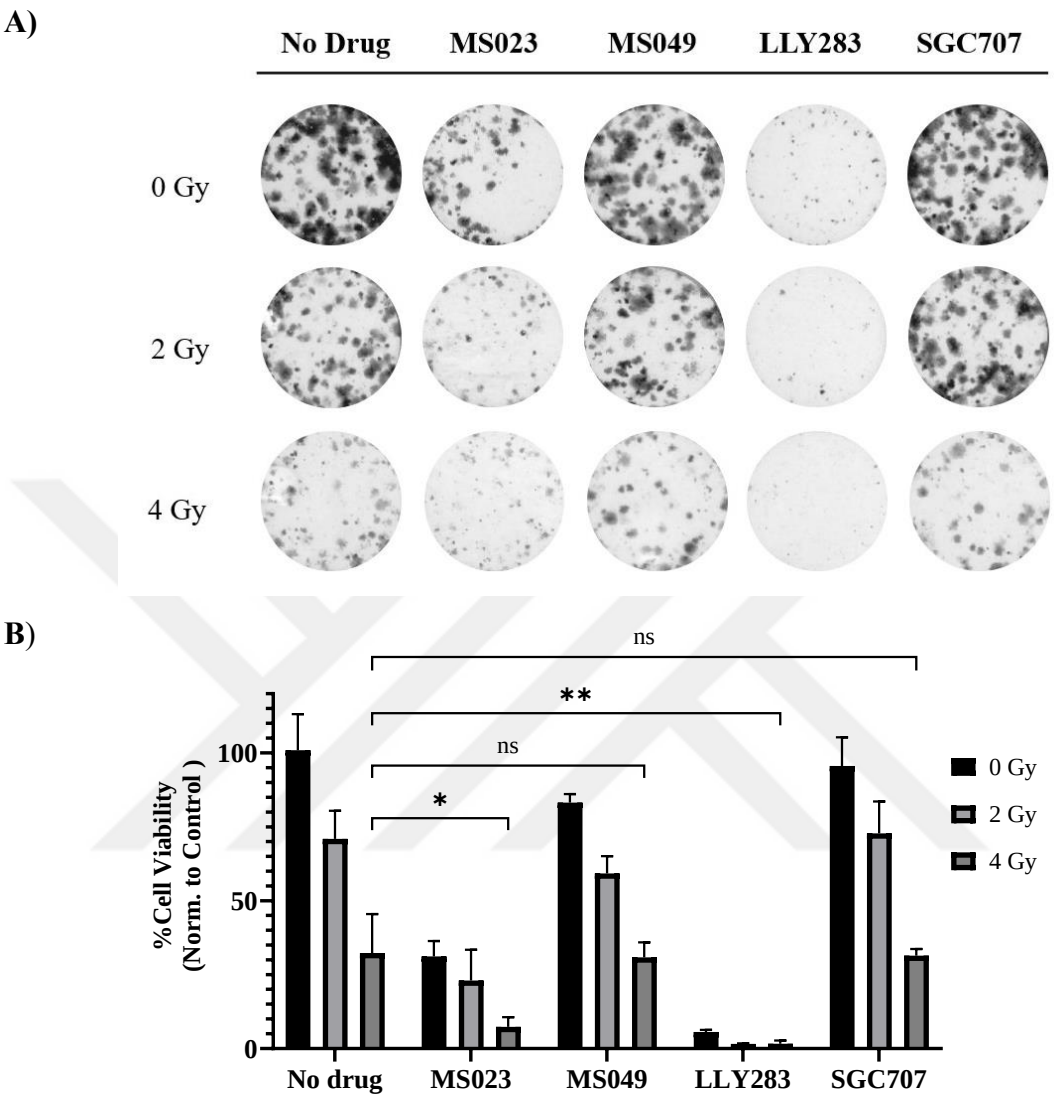

Figure 3.3.1 Effect of PRMT inhibitor (24 h pretreatment) and/or IR on U373 cells. **A)** Representative images of clonogenic assay of U373 cells with the combination of drug and radiation. **B)** Quantification of colony numbers. * $p<0.05$, ** $p<0.005$

Accordingly, 24-hour pre-treatment with LLY283 and MS023 at the indicated doses was effective in reducing cell growth, but MS049 and SGC707 by themselves did not reduce growth in the absence of radiation. When drugs and radiation was combined, the effect of radiation was prominent, regardless of the drug treatment.

3.3.2 Testing the effect of 48 h pre-treatment

To study the effects of selected drugs further, longer pre-treatment times were tested. After a 48-hour pre-treatment, cells were exposed to 2 and 4 Gy radiation and colony-forming ability was measured after 14 days as illustrated in **Figure 3.3.2**.

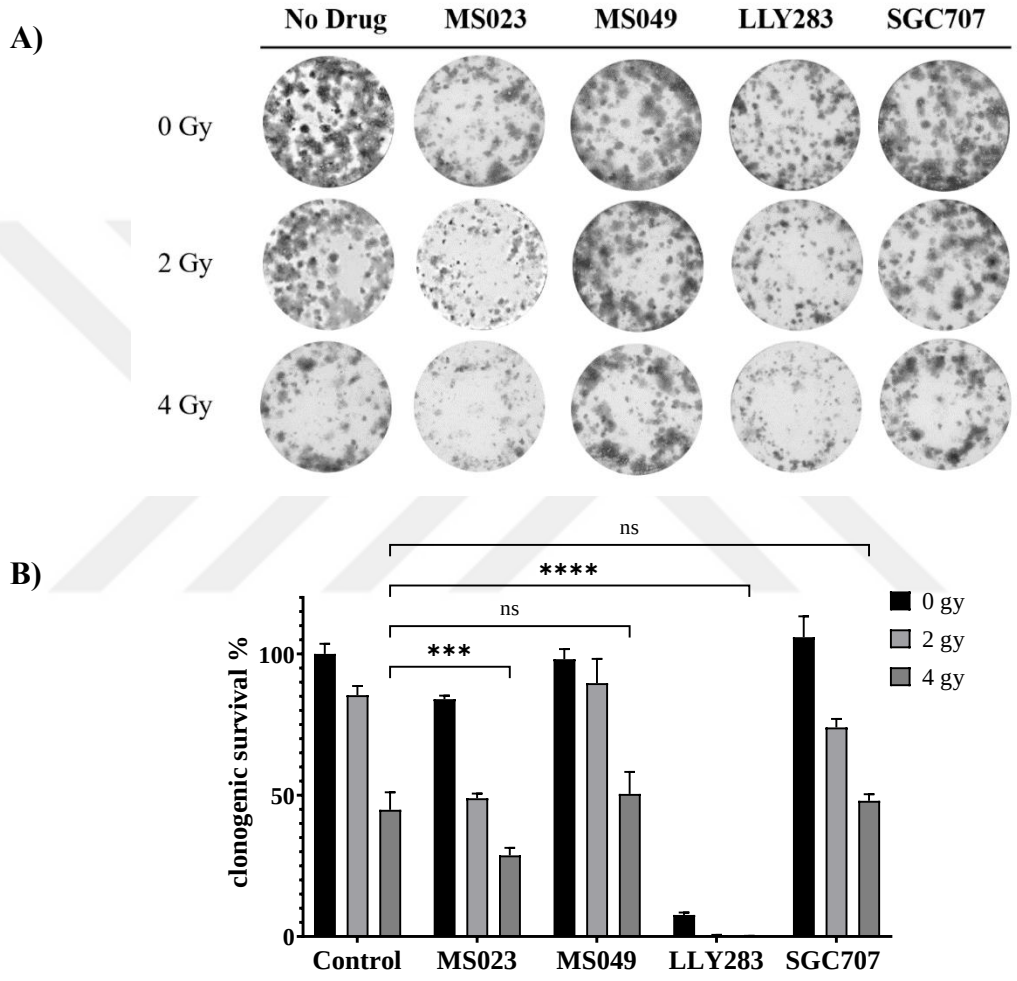

Figure 3.3.2 Effect of PRMT inhibitor (48h pretreatment) and/or IR on U373 cells. **A)** Representative images of clonogenic assay of U373 cells with the combination of drug and radiation. **B)** Quantification of colony numbers. *** p< 0.001, **** p<0.0001

According to these results, LLY283 was toxic on its own, in line with our previous observations. MS023 by itself did not cause toxicity but when combined with 4 GY radiation, a significant reduction in cell growth was observed, compared to either treatment alone (**Figure 3.3.2)**

3.3.3 Testing the effect of 72 h pre-treatment

U373 GBM cells were treated for 72 hours and then received 2 - 4 Gy radiation. This result shows that compared to only RT, cells showed a greater response to radiation and fewer colony-forming abilities than their control groups as a result of combined treatment with a PRMT inhibitor (**Figure 3.3.3)**

A)

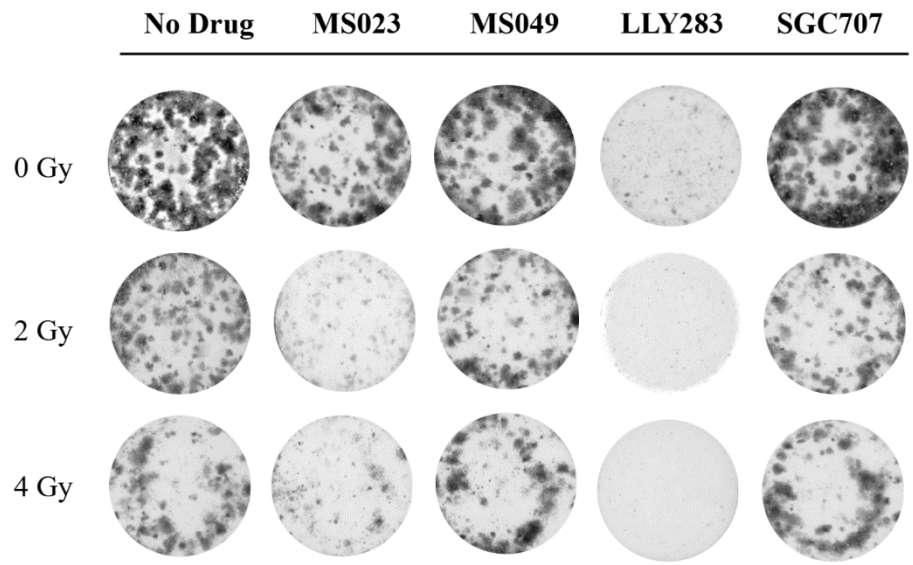

B)

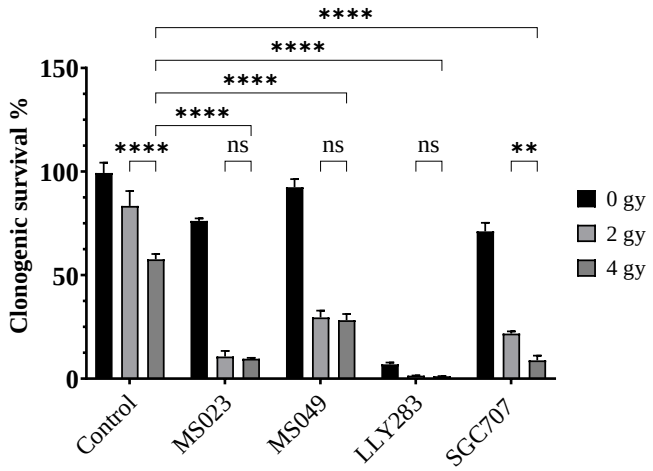

Figure 3.3.3 Effect of PRMT inhibitor (72h pretreatment) and/or IR on U373 cells. **A)** Representative images of clonogenic assay of U373 cells with the combination of drug and radiation. **B)** Quantification of colony numbers. **** $p<0.0001$

As a result of the optimization between drug treatment and radiation, it was observed that the combination of MS023, with a 48-hour pre-incubation period, and 4 Gy radiation exhibited a cooperative effect on U373 cells compared to radiation alone. This finding underscores the potential impact of MS023 in enhancing the radiosensitivity of U373 GBM cells. The subsequent phase of the thesis delves into a detailed exploration of the molecular changes of MS023 on cellular pathways.

3.3.4 Testing the Effect of PRMT Inhibition on Dimethylarginine Expression

To investigate whether PRMT inhibition in U373 cells changes arginine methylation, we first used western blotting to detect the overall levels of symmetric dimethylarginine (SDMA) in cells upon inhibitor treatments. The results showed that the levels of SDMA in U373 cells were significantly decreased after MS023 and LLY283 treatment.

In an experimental setup, U373 cells were subjected to treatment with 2 mM concentrations of MS023, MS049, SGC707, and 1uM LLY283 drugs. Following this treatment, cells were incubated for 48 hours and subsequently exposed to 4 Gy of irradiation. The cells were harvested 24 hours after the IR treatment. In the nuclear fractionation process, it was observed that LLY283, which targets PRMT5 enzyme activity, led to a reduction in enzyme activity as illustrated in **Figure 3.3.4**. This reduction was indicated by a decrease in the expression of SDMA.

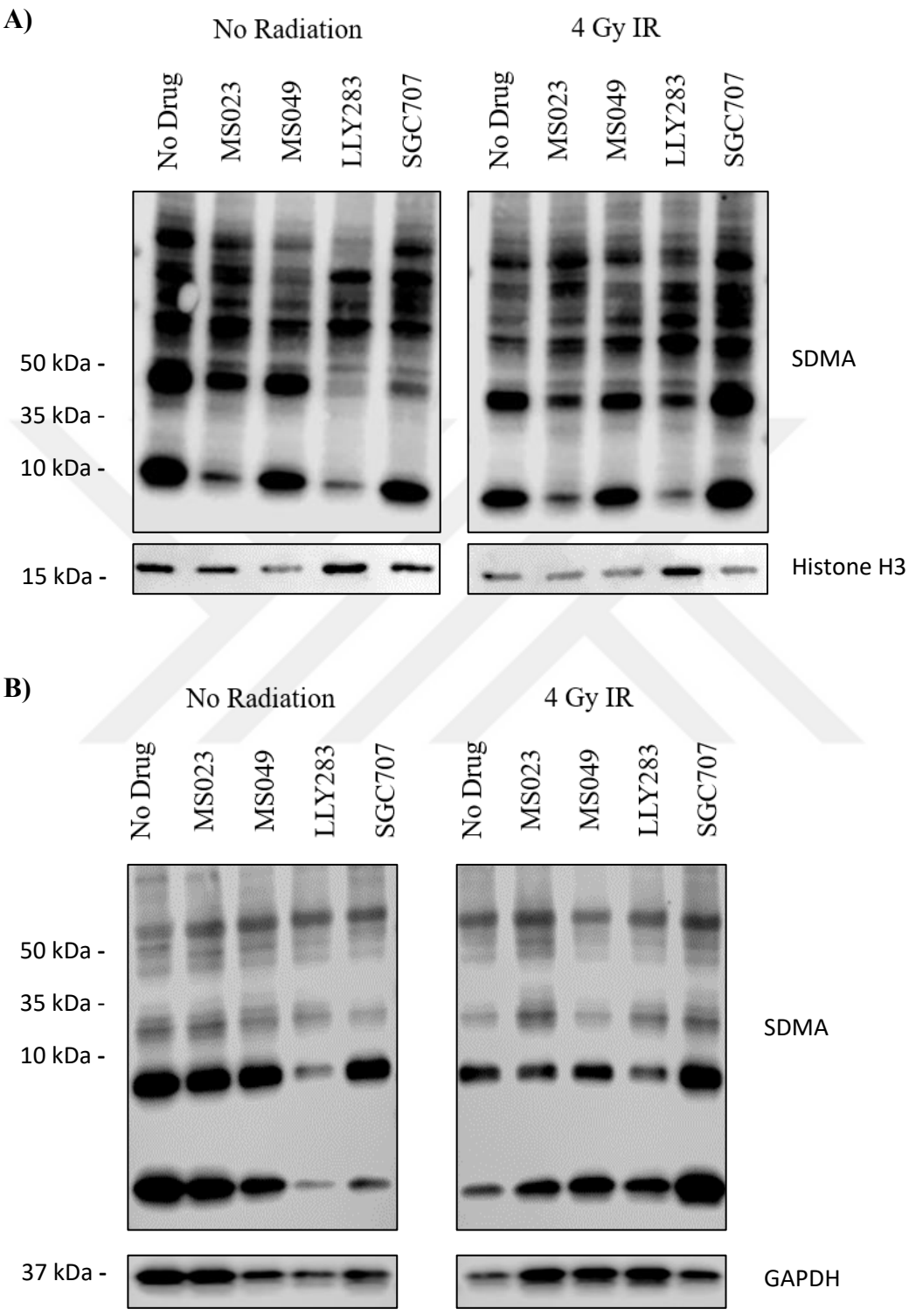

Figure 3.3.4 Western blot of symmetric dimethylarginine (SDMA) in U373 cells. **A)** SDMA expression in U373 cells exposed to IR and treated with PRMT inhibitors, followed by nuclear fractionation. **B)** SDMA expression in U373 cells exposed to IR and treated with PRMT inhibitors, followed by cytosolic fractionation.

3.4 Proliferation of PRMT Knockdown Using CRISPR/Cas9 in U373 Cas9 Stable Cell Line

To study the effect of PRMT inhibition in radiation response of GBM using a complementary genetic approach, we employed CRISPR/Cas9 system to silence the expression of PRMT encoding genes. For this purpose, gRNAs targeting PRMTs were cloned in lentiviral backbones and the lentivirus was introduced to into U373-Cas9 stable cell line. Samples were collected following puromycin selection. After 5 days of selection, significant depletion upon knockout of essential genes was observed, while there was no change in non-targeting controls as gauged by qRT-PCR.

As illustrated in **Figure 3.4.1**, a decrease in mRNA levels is observed in cell lines generated using guides designed for PRMT1, compared to the non-targeting control group. Notably, the reduction in expression of PRMT1 was more notable with PRMT1 g1 and PRMT1 g3 (**Figure 3.4.1)** The results of a 10-day colony formation experiment indicate a significantly lower survival potential in the PRMT1g1 and g3 groups; where colony growth was significantly inhibited compared to NT transduced cells. In contrast, the PRMT1 g2 group exhibits a reduced capacity for colony formation; and this was accentuated upon IR-treatment (**Figure 3.4.1 B-C)**.

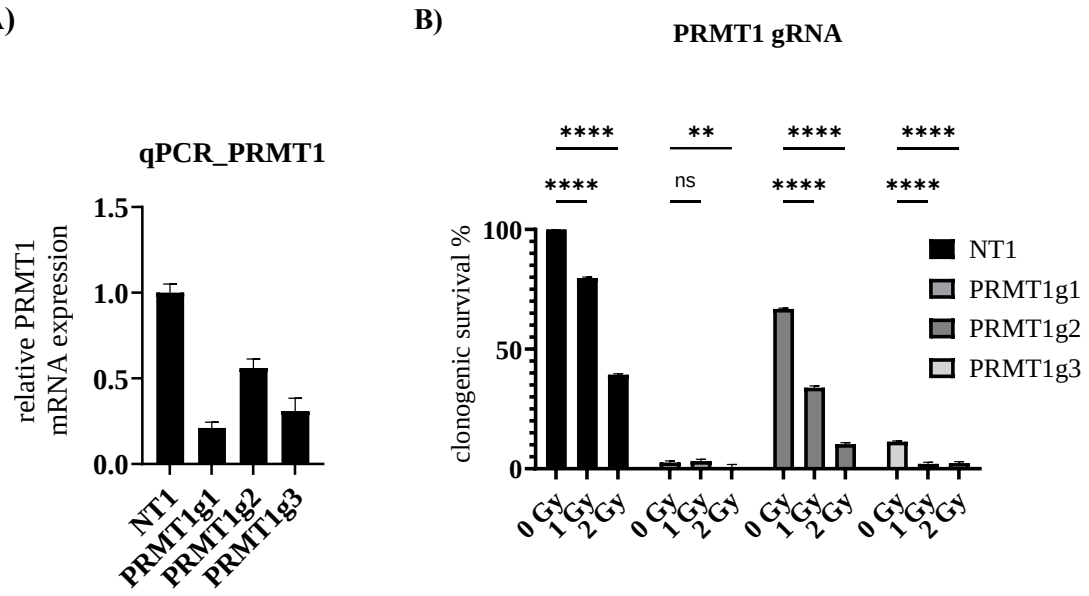

C)

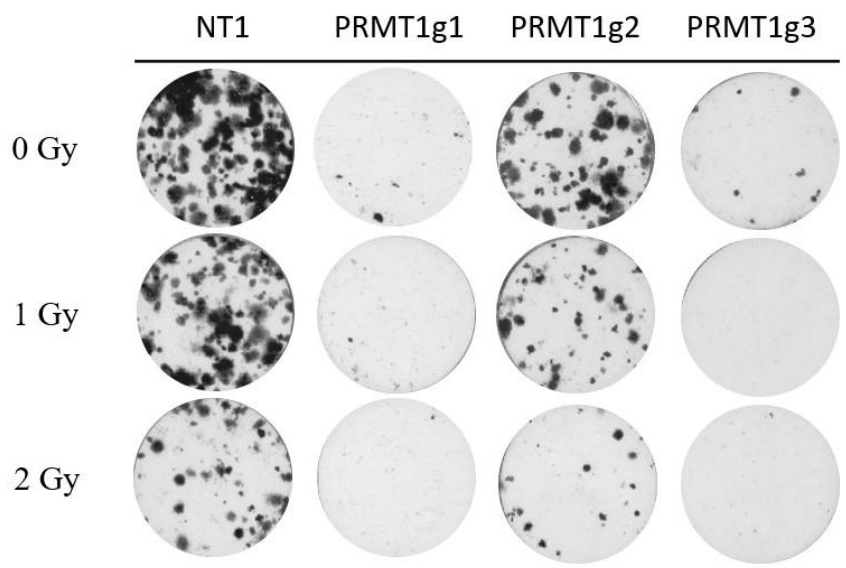

Figure 3.4.1 Effect of PRMT1 CRISPR/Cas9 on U373 cells. **A)** mRNA expression levels of PRMT1 normalized to the NT1. **B)** Quantification of colony numbers. **C)** Representative images of clonogenic assay. ** $p<0.005$, *** $p< 0.001$, **** $p<0.0001$

As illustrated in **Figure 3.4.2**, a decrease in mRNA levels is observed in cell lines generated using guides designed for PRMT3, compared to the non-targeting control group. Furthermore, the results of a 10-day colony formation experiment indicate no marked change in the survival potential of the PRMT3 g groups compared to the control group. Specifically, the combination of PRMT3 g3 with 2 Gy IR resulted in a significant reduction in the capacity for colony formation in cells.

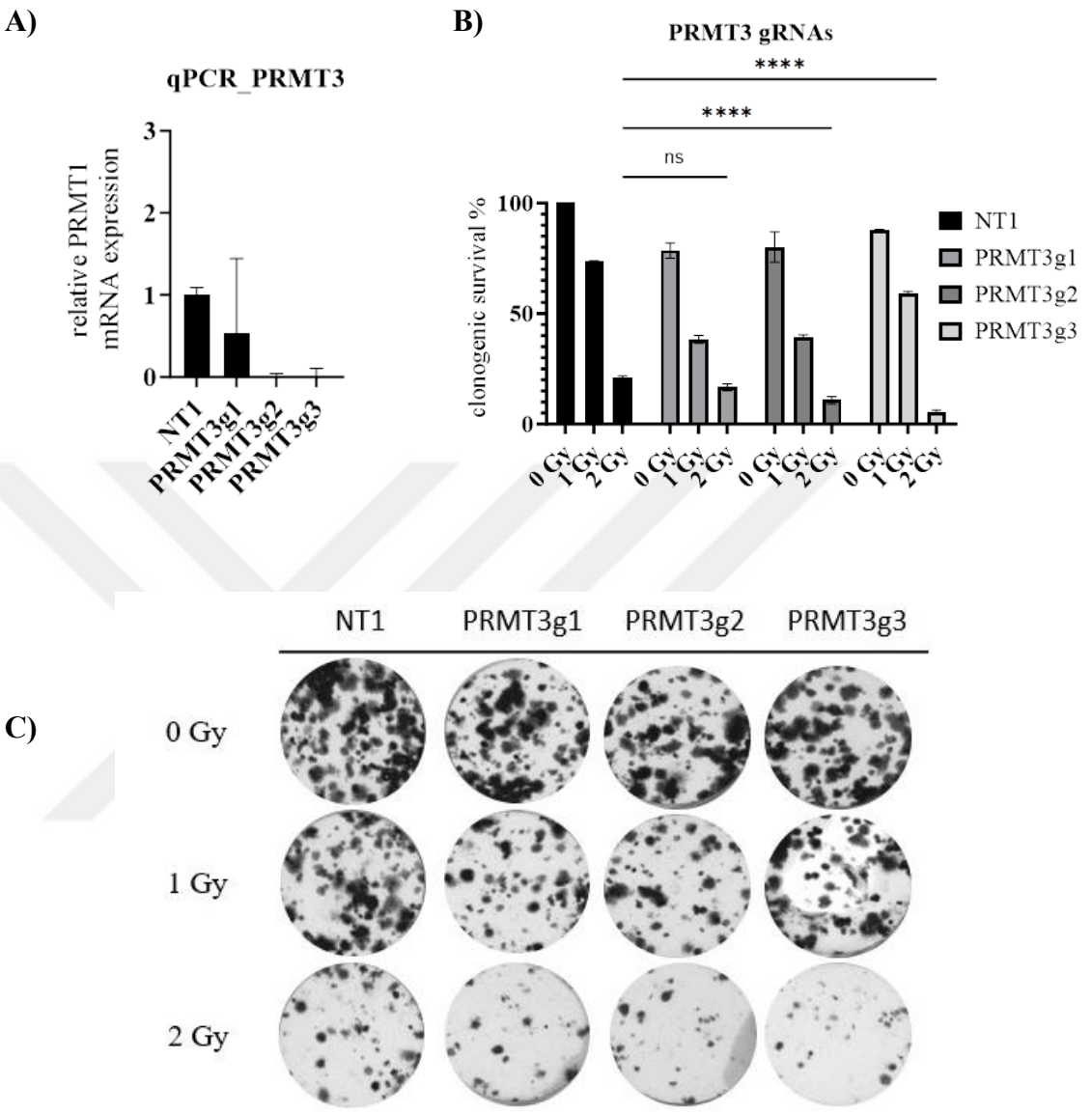

Figure 3.4.2 Effect of PRMT3 CRISPR/Cas9 on U373 cells. **A)** mRNA expression levels of PRMT3 normalized to the NT1**. B)** Quantification of colony numbers. **C)** Representative images of clonogenic assay **** $p<0.0001$

The generated PRMT5 knockout cells were validated through qPCR at mRNA levels in **Figure 3.4.3**. Notably, PRMT5 g1 and g2 had significantly lower expression levels compared to NT1. Consequently, the observed substantial reduction in cell survival strongly indicates the significant impact on cell viability resulting from the depletion of the essential gene PRMT5.

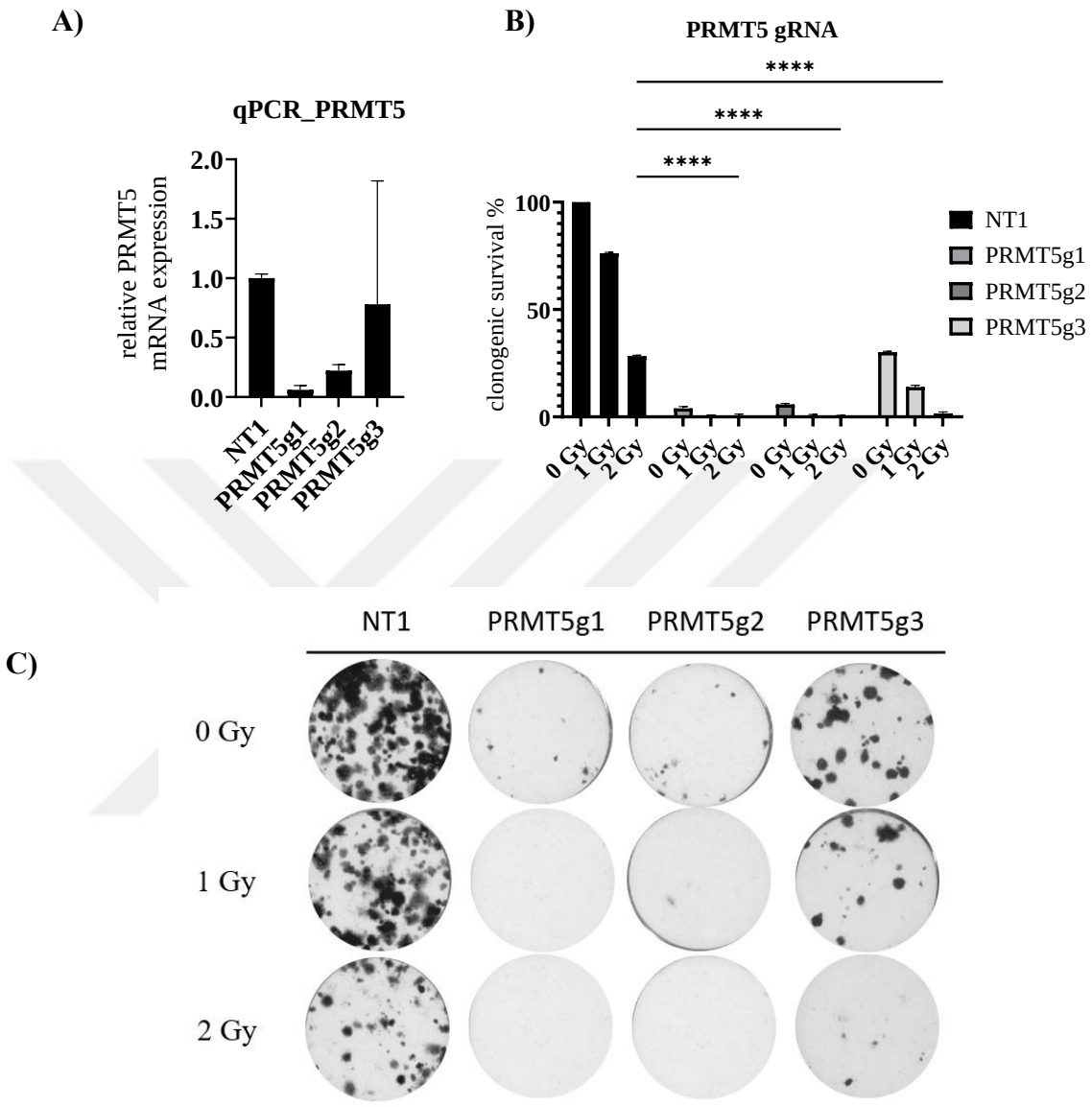

Figure 3.4.3 Effect of PRMT5 CRISPR/Cas9 on U373 cells. **A)** mRNA expression levels of PRMT5 normalized to the NT1. **B)** Quantification of colony numbers. **C)** Representative images of clonogenic assay ****p<0.0001

A)

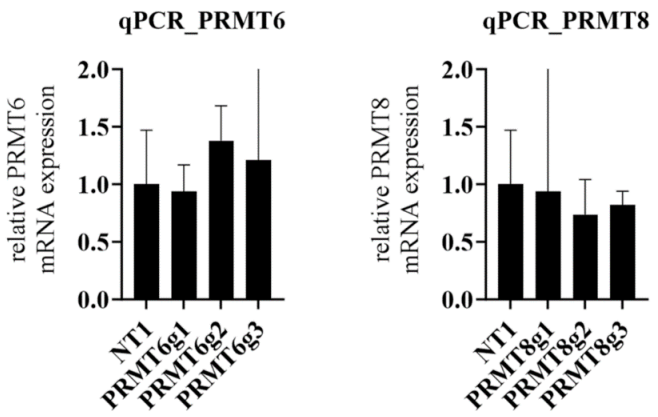

B)

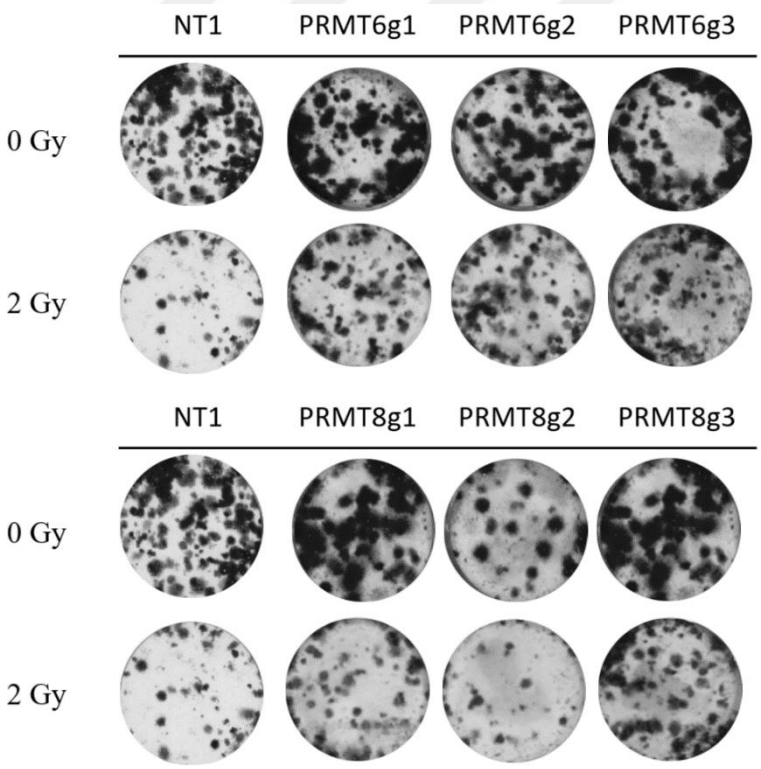

Figure 3.4.4 Effect of PRMT6 and PRMT8 CRISPR/Cas9 on U373 cells. **A)** mRNA expression levels of PRMT6 and PRMT8 normalized to the NT1. **B)** Representative images of clonogenic assay.

As seen in **Figure 3.4.4**, knockout cells could not be generated for PRMT6 and PRMT8 as there was no notable drop in their mRNA expression. In a parallel experiment that was set up, there was no phenotype associated with gRNA transduction, where all cells were similar to NT groups. Future work will be continued to optimize the experiments with PRMT6 and PRMT8.

3.5 Exploring Transcriptional Changes Induced by MS023 and/or IR in U373 Cells Through RNA Sequencing

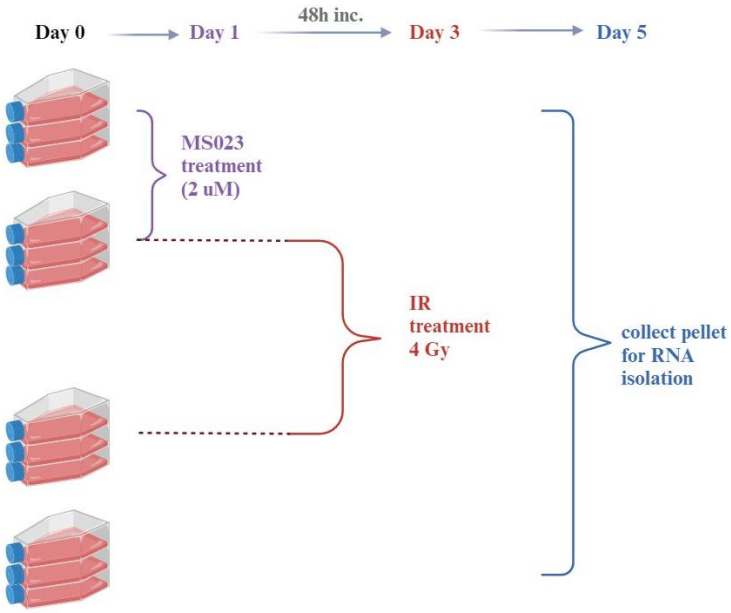

Figure 3.5.1 Experimental approach for analyzing transcriptomic changes upon MS023 and/or IR treatment.

Our results above revealed that a combination of MS023 and a single dose IR works efficiently on U373 cells; especially when drug application is performed for 48 hours before IR application. To investigate changes in the transcriptome of GBM cells upon drug and/or IR treatment, we undertook RNA sequencing and repeated the experiment on larger scale to collect samples for profiling **(Figure 3.5.1).**

As it is very important to ensure that samples prepared for sequencing are indeed coming from a successful experiment, we set up a parallel experiment to test the colony formation ability of samples treated with drug and/or IR (**Figure 3.5.2).** Evaluation of cell survival outcomes initiated from cells treated with MS023 alone revealed a significantly reduced potential for colony formation compared to the control group, underscoring the impact of MS023 on cellular proliferation. Notably, in comparison to cells treated only with 4 Gy irradiation, the combination treatment of MS023 and 4 Gy led to a further reduction in colony numbers and cell viability. Given the results showing the efficacy of combined MS023 and IR, we sent all replicas to RNA sequencing.

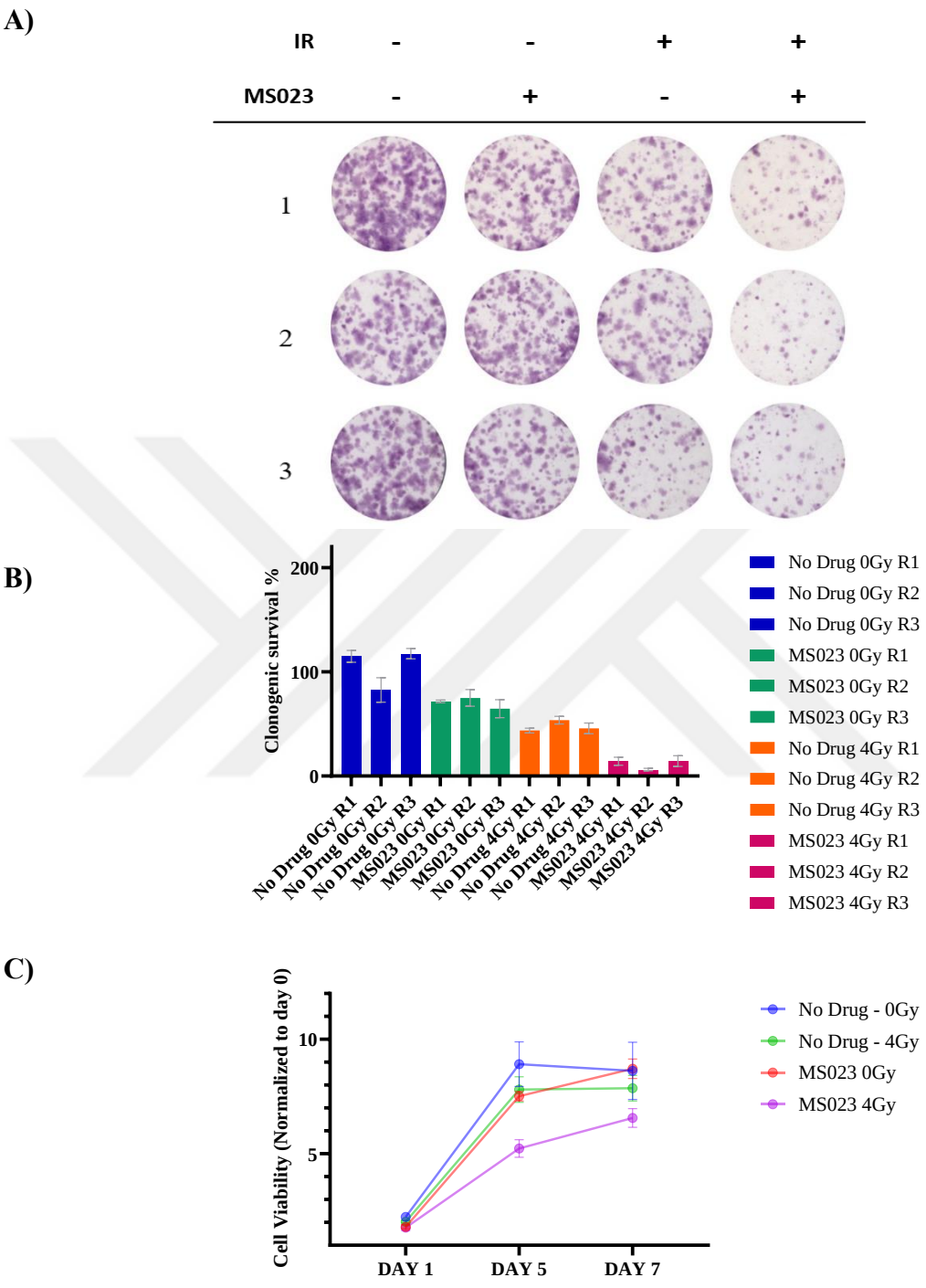

Figure 3.5.2 Cell viability upon MS023 and/or IR treatment, on samples sent for RNA sequencing. (n=3 for each treatment, R1, R2, R3: replicate numbers). **A)** Representative images of the clonogenic assay. **B)** Quantification of colony numbers. **C)** Cell viability assay by CTG.

3.5.1 Transcriptomic Profiling Reveals Altered Gene Expression in MS023-Treated U373 Cells

To investigate the impact of type-I PRMT inhibition on transcriptomic changes in the U373 GBM cells, cells treated with 2 mM MS023 for 72h and/or IR were evaluated by RNA sequencing in triplicates.

PCA analysis revealed different clustering patterns between MS023 treated and non-treated samples; this indicates distinct gene expression profile changes. Specifically, it indicates a higher similarity within the group (**Figure 3.5.1.1**). In total 7189 genes were differentially expressed upon MS023 treated, 3570 of them were upregulated and 3619 of the genes were downregulated. Volcano plots of differentially expressed genes are shown in **Figure 3.5.1.1**. Some of the significant upregulated genes were *NDRG1, SERPINE1, ALDOA*, *NUPR1, DDIT4, CITED1, CITED2, RCC1,* and *HIF1*, associated with hypoxia regulation. The downregulation was observed in genes associated with DNA damage response and repair, including *RFC4, MPG*, and *POLD1*, as well as cell cycle regulated and G2M cell checkpoint including *FOXN3, AURKA, TOP2A, PRC1, Cyclin 1-2-6*, E2Fs and MYC target genes.

Gene Set Enrichment Analysis (GSEA) of the RNA-seq data report showed that G2M Checkpoint (NES: -2.36), E2F Targets (NES: -2.51), and DNA Repair (NES: -2.16) pathways dipslayed negative enrichment, suggesting potential regulation of these pathways. Conversely, Hypoxia (NES: 2.18), TNFA signaling via NFKB (NES: 2.13), and UV Response Up (NES: 1.19) showed positive enrichment, in the hallmark pathways (**Figure 3.5.1.2**).

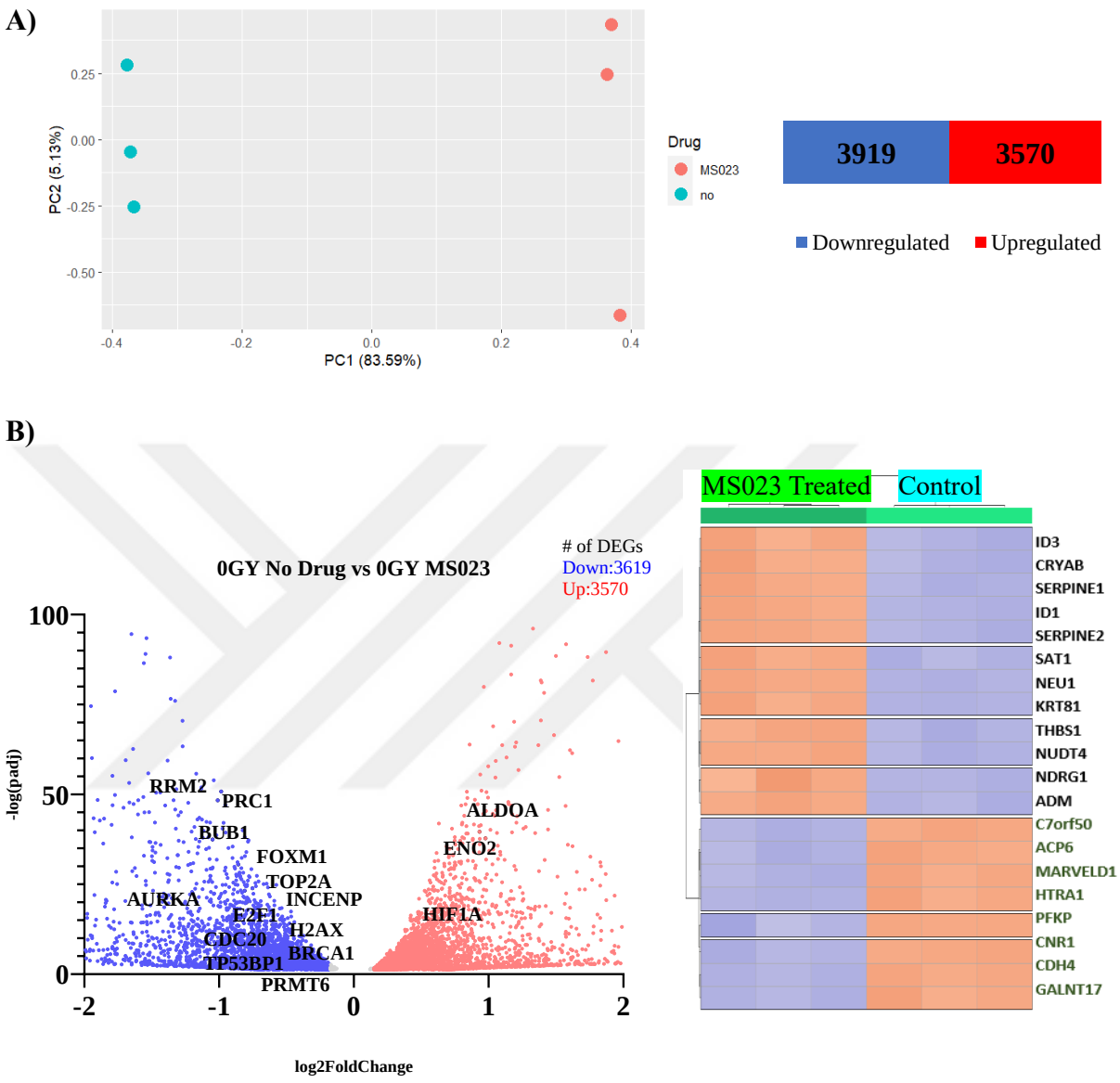

Figure 3.5.1.1 RNA-seq analysis for MS023 treated and non-treated U373. **A)** PCA plot and numbers of differentially expressed genes. **B)** Volcano plot and top 20 differential genes.

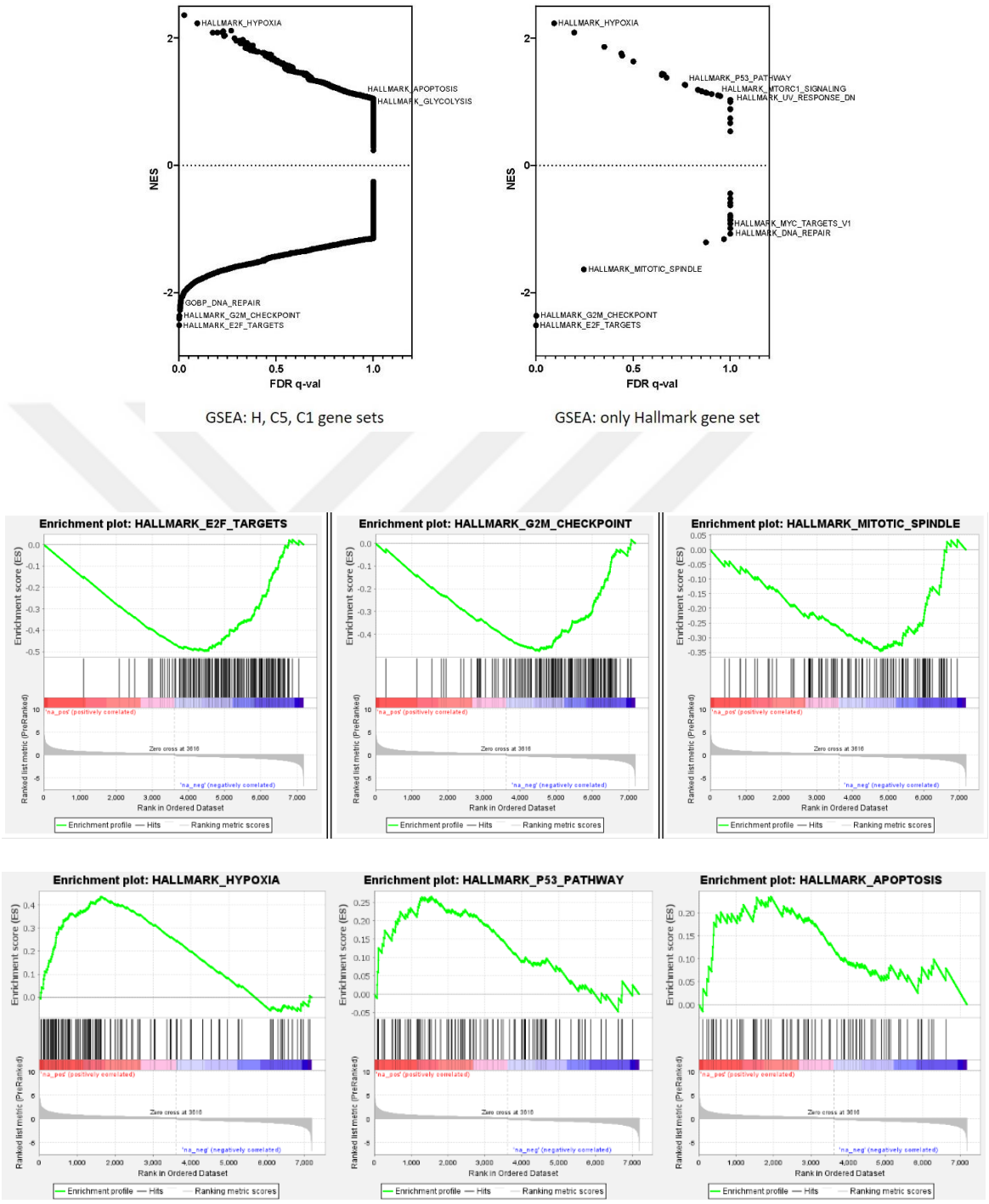

Figure 3.5.1.2 Gene Set Enrichment Analysis (GSEA) and representative enrichment plots of U373 cells treated MS023.

3.5.2 RNA Sequencing Analysis of Radiation-Treated U373 Cells

To investigate the impact of irradiation on transcriptomic changes in the U373 GBM cells, cells treated with 4 Gy in triplicates. RNA sequencing was performed on the collected cells, and cell viability assays by clonogenic and CTG were also established with these collected cells. According to the results, the impact of the IR on cell survival has been demonstrated and resulted in a significant decrease.

PCA analysis revealed different clustering patterns between IR-treated and non-radiated samples; this indicates distinct gene expression profile changes. Specifically, it indicates a higher similarity within the control (non-treated) group **(Figure 3.5.2.1)**. In total 230 genes were differentially expressed upon irradiation, 85 of them were downregulated and 145 of the genes were upregulated. Volcano plots of differentially expressed genes are shown in **Figure 3.5.2.2** The significant upregulation some genes are CCNB1, KIF20A, AURKA, FOXM1, TOP2A. The downregulation was observed in genes PDE1C, NUPR1, and MCM6.

Gene Set Enrichment Analysis (GSEA) of the RNA-seq data report showed that G2M Checkpoint (NES: -1.61), E2F Targets (NES: -1.71), and mitotic spindle (NES: -1.98 pathways are negative enrichment. Due to the downregulation of several histone methylations, multiple negatively enriched gene sets were identified including GO genets. There are microtubule organization (NES: -2.42), cell cycle process (NES:-2.40), and cell division (NES: -2.36).

A)

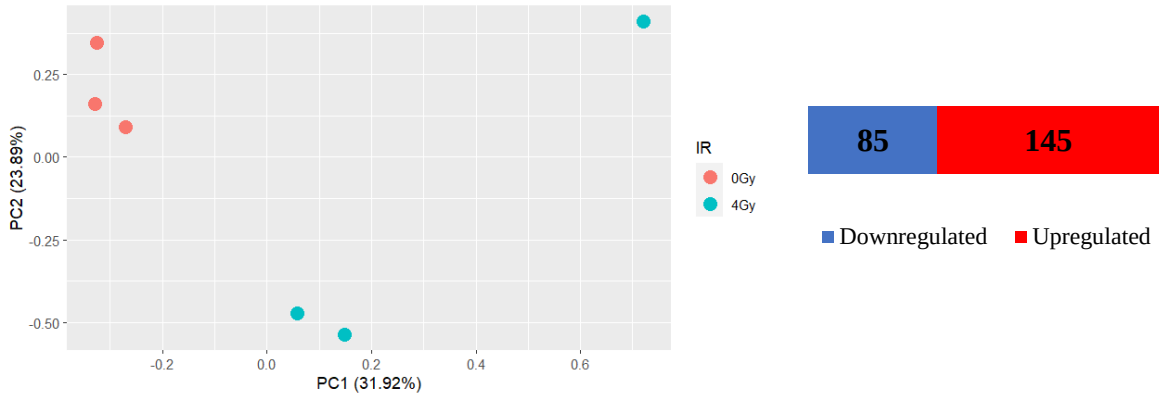

B)

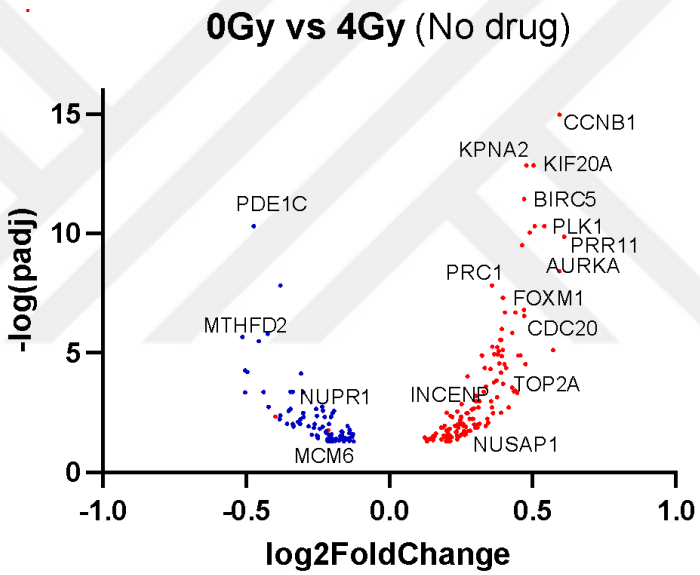

Figure 3.5.2.1 RNA-seq analysis for irradiated with 4 Gy and non-treated U373. **A)** PCA plot and numbers of differentially expressed genes. **B)** Volcano plot of transcriptome profiles of radiated GBM cells.

	GS follow link to MSigDB	GS DETAILS	SIZE	ES	NES	NOM p-val	FDR q-val
1	GOBP_MICROTUBULE_CYTOSKELETON_ORGANIZATION	Details ...	46	-0.64	-2.42	0.000	0.097
2	GOCC_SPINDLE_POLE	Details ...	20	-0.72	-2.40	0.000	0.082
3	GOBP_CELL_CYCLE_PROCESS	Details ...	75	-0.60	-2.40	0.000	0.059
4	GOBP_NUCLEAR_CHROMOSOME_SEGREGATION	Details ...	43	-0.64	-2.36	0.000	0.097
5	GOBP_CELL_DIVISION	Details ...	60	-0.61	-2.34	0.000	0.126
6	GOCC_SPINDLE	Details ...	43	-0.61	-2.34	0.000	0.109
7	GOBP_MICROTUBULE_BASED_PROCESS	Details ...	49	-0.61	-2.31	0.000	0.152
8	GOBP_MITOTIC_CELL_CYCLE_PROCESS	Details ...	67	-0.57	-2.29	0.000	0.192
9	GOBP_NON_MEMBRANE_BOUNDED_ORGANELLE_ASSEMBLY	Details ...	24	-0.65	-2.28	0.009	0.188
10	GOBP_CHROMOSOME_SEGREGATION	Details ...	47	-0.61	-2.27	0.000	0.205
11	GOBP_ORGANELLE_FISSION	Details ...	46	-0.59	-2.26	0.000	0.225
12	GOBP_CELL_CYCLE	Details ...	90	-0.54	-2.23	0.000	0.345
13	GOBP_CYTOSKELETON_ORGANIZATION	Details ...	59	-0.57	-2.21	0.000	0.367
14	GOBP_SISTER_CHROMATID_SEGREGATION	Details ...	37	-0.60	-2.20	0.000	0.393
15	GOBP_SPINDLE_ORGANIZATION	Details ...	28	-0.66	-2.20	0.000	0.374
16	GOBP_MICROTUBULE_CYTOSKELETON_ORGANIZATION_INVOLVED_IN_MITOSIS	Details ...	27	-0.62	-2.16	0.007	0.522
17	GOCC_MICROTUBULE_CYTOSKELETON	Details ...	62	-0.55	-2.16	0.000	0.519
18	GOBP_MITOTIC_SISTER_CHROMATID_SEGREGATION	Details ...	34	-0.60	-2.14	0.002	0.556
19	GOBP_SPINDLE_ASSEMBLY	Details ...	19	-0.64	-2.14	0.090	0.556
20	GOBP_CHROMOSOME_ORGANIZATION	Details ...	47	-0.57	-2.13	0.000	0.536

Figure 3.5.2.2 Negative enrichment of GO genesets upon U373 GBM cells irradiated 4 Gy.

3.5.3 RNA Sequencing Analysis of MS023 and Radiation-Treated U373 Cells

To assess the impact of irradiation on transcriptomic changes in MS023-treated U373 GBM cells when combined with 4 Gy radiation, cells were treated with MS023 for 48h and then received 4 Gy in triplicates. Subsequently, RNA sequencing and cell viability assays (clonogenic and CTG) were conducted on the collected cells. The results demonstrated a significant decrease in cell survival upon irradiation.

PCA analysis revealed distinct clustering patterns between irradiation-treated and non-radiated samples, indicating notable changes in gene expression profiles (**Figure 3.5.3.1**). A total of 7125 genes exhibited differential expression upon irradiation, with 3589 downregulated and 3536 upregulated genes. Volcano plots illustrating differentially expressed genes are presented in **Figure 3.5.3.1**. Noteworthy upregulation was observed in genes such as *CCNB1, CDK1, BUB1, KIF4A, PLK1* and *AURKA*, while downregulation was noted in genes like *GAPDH, SERPINE1, NDRG1* and *DEPP1*. These findings highlight the significant impact of irradiation on the transcriptomic landscape and provide insights into specific genes affected by the treatment.

A)

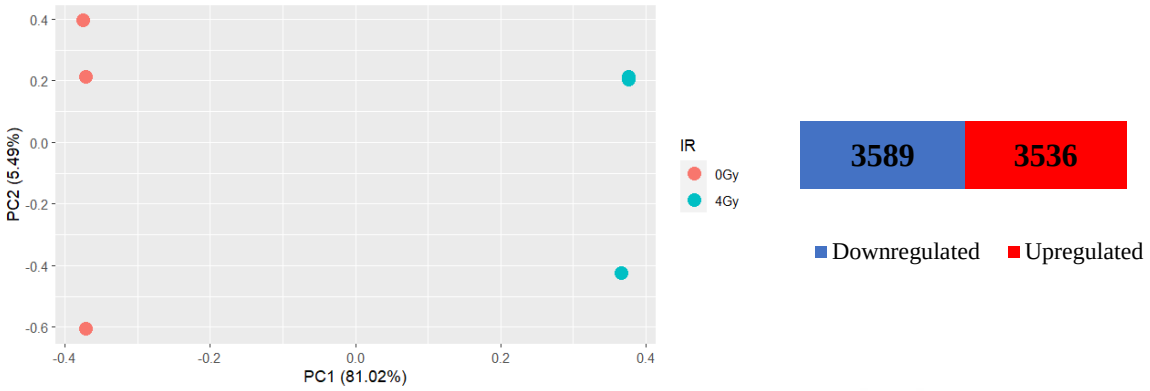

B)

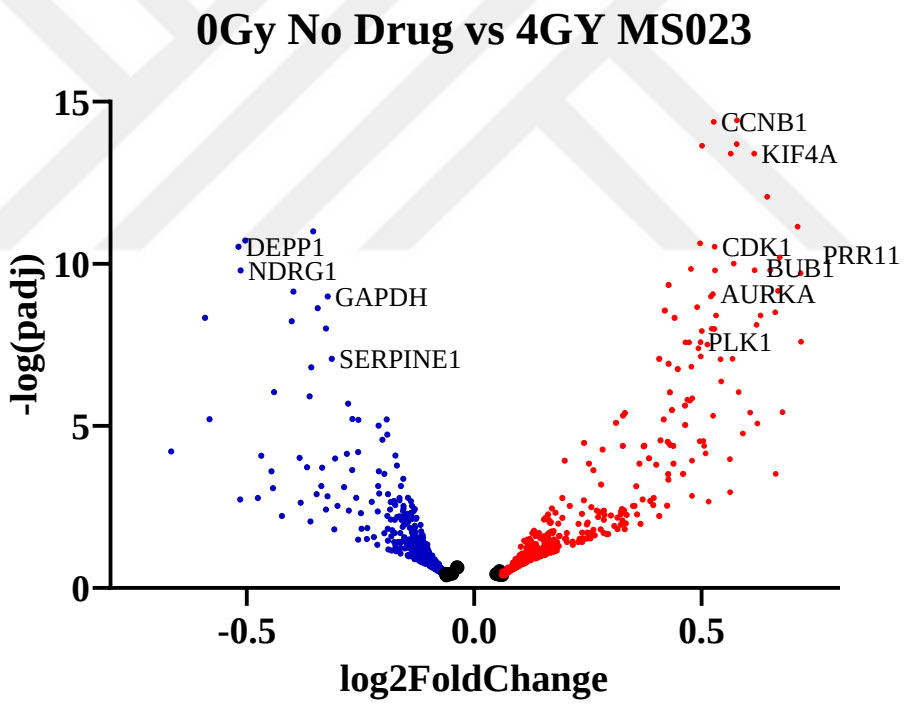

Figure 3.5.3.1 RNA-seq analysis for MS023 treated and irradiated with 4 Gy and non-treated and non-radiated U373. **A)** PCA plot and numbers of differentially expressed genes. **B)** Volcano plot of analysis.

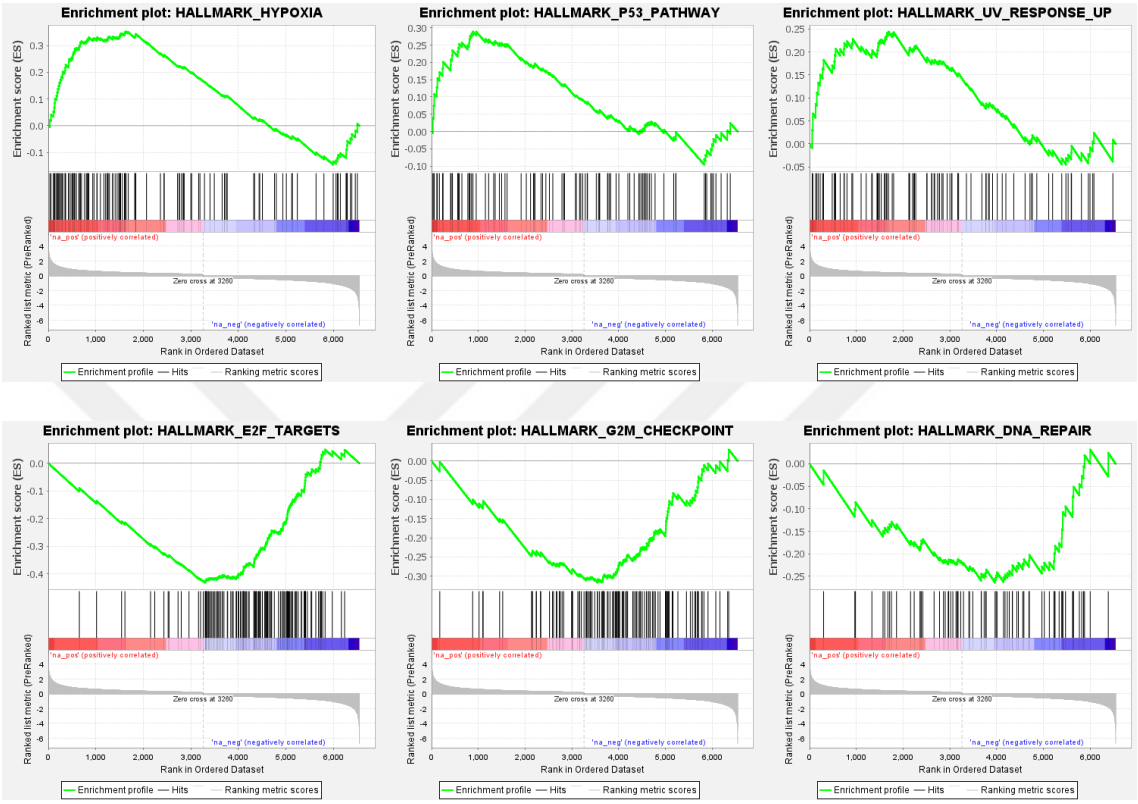

Figure 3.5.3.2 Gene Set Enrichment Analysis (GSEA) and representative enrichment plots of U373 cells treated MS023 and irradiated 4 Gy.

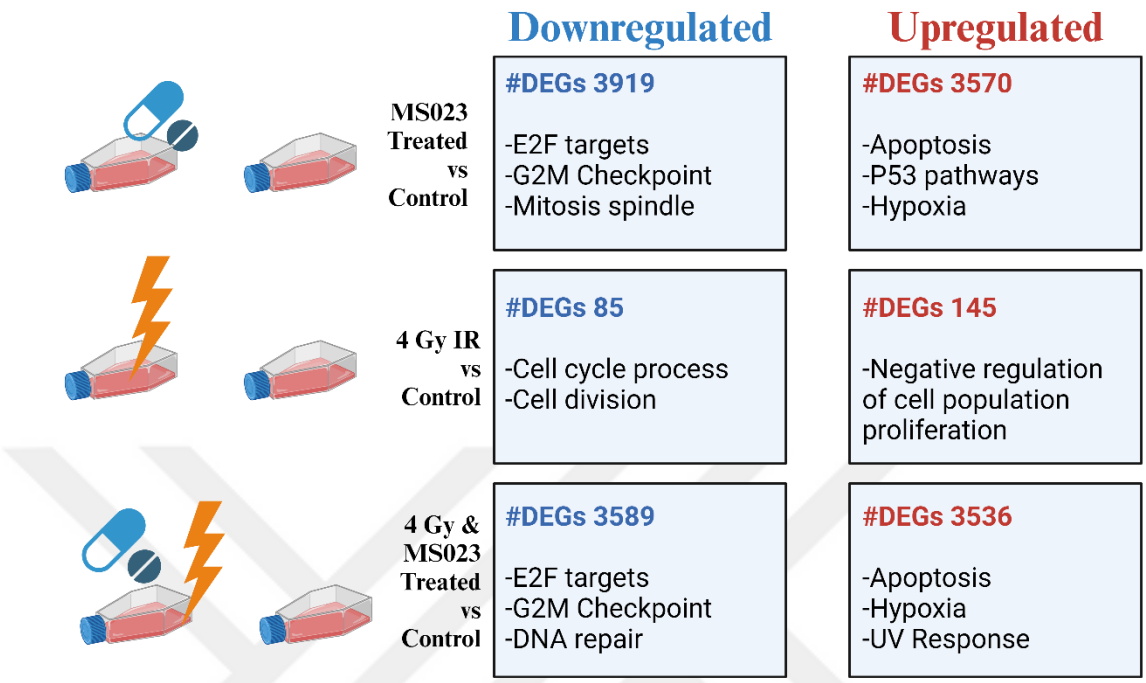

Figure 3.5.3.1 Summary of RNA sequencing results, showcasing the differential gene numbers and related pathways identified through GSEA analysis..

3.6 Investigation of PRMT Inhibition on IR-Induced activated H2AX Effects

The activated form of H2AX was examined using the pH.2AX assay kit to investigate the impact of PRMT inhibition on IR-induced phosphorylated H2AX. U373 cells were incubated with 2 μM MS023 and 1 μM LLY283 drugs for 48 hours. Subsequently, they were treated with 4 Gy IR, and cells collected at 1, 3, and 6 hours post-treatment were analyzed for activated H2AX using flow cytometry, as illustrated in **Figure 3.6**. According to the results, only IR treatment resulted in a significant activation of H2AX at the end of the first hour. In contrast, cells treated with the drug showed a less pronounced expression of activated H2AX following IR.

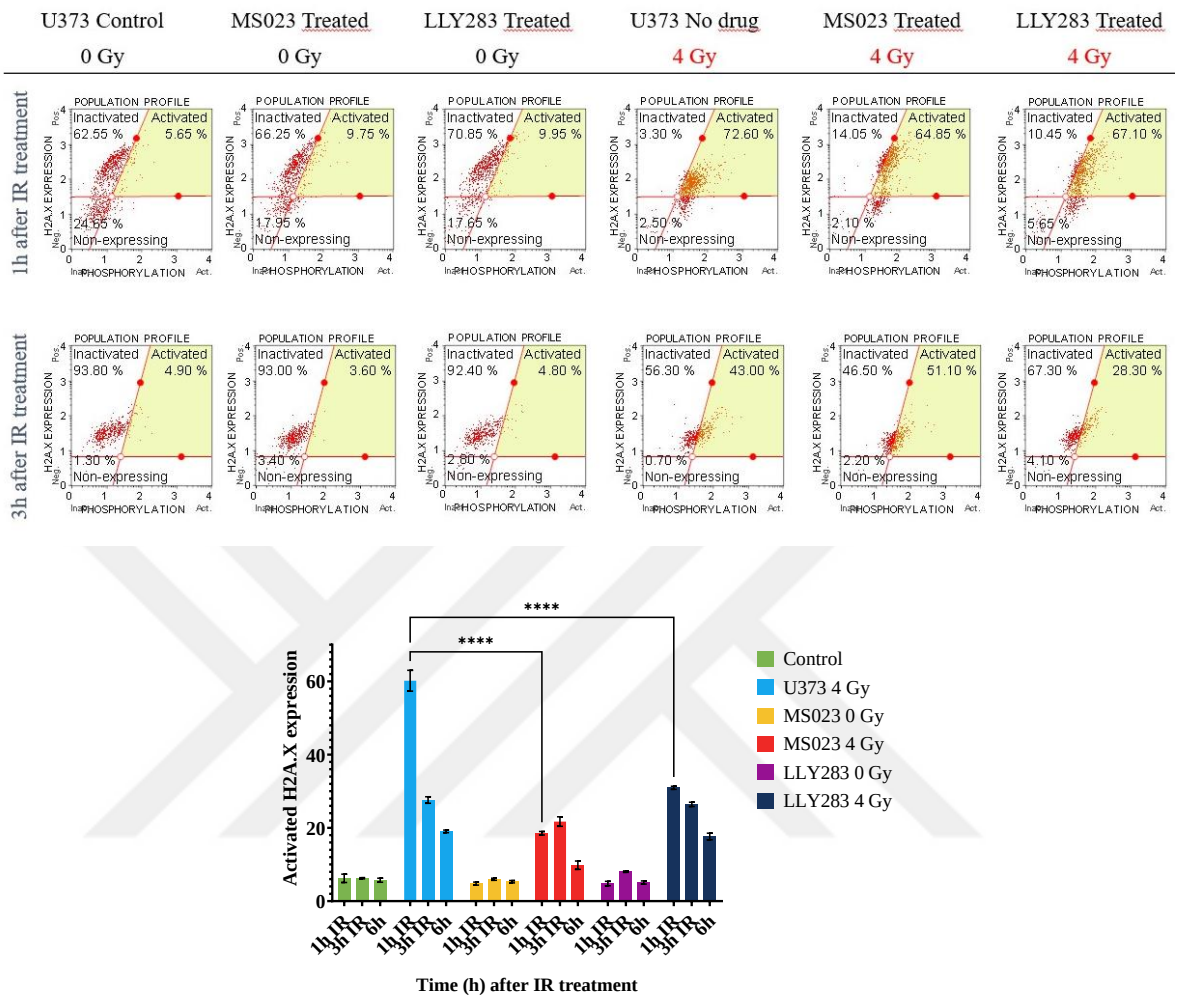

Figure 3.6 The activation of γ-H2AX in U373 cells following treatment with MS023 and LLY283 in combination with 4 Gy ionizing radiation (IR).

Chapter 4: **DISCUSSION**

Glioblastoma, the most prevalent and aggressive brain tumour in adults, is characterized by a high recurrence rate and limited survival. The recurrent nature of GBM is primarily attributed to the tumour cells' remarkable ability to adapt and develop resistance to conventional treatments. Radiotherapy stands out as a traditional approach, yet gliomas often exhibit a suboptimal response to ionizing radiation, necessitating a deeper exploration of the molecular mechanisms that underscore radioresistance.

A comprehensive analysis of the molecular mechanisms underlying radiation-induced cellular changes is crucial for a better understanding of the complex processes leading to radioresistance. Although genetic alterations play a pivotal role in cancer progression, the significance of epigenetic modifications in orchestrating gene expression patterns is equally noteworthy. Post-translational modifications, particularly methylation, play critical roles in the landscape of brain tumorigenesis. This multifaceted exploration unveils the intricate interplay between epigenetic factors and radiation response, offering valuable insights into potential therapeutic interventions.

In this thesis, we conducted a thorough investigation into the effects of protein arginine methylation inhibitors on GBM cells to understand their impact on cell behavior. Our goal was to explore how PRMT inhibition influences the response of GBM cells to radiation, revealing potential therapeutic implications. Initially, we disrupted PRMT enzyme activity systematically using selective chemical inhibitors and examined the response of the GBM cell line U373 to the combined treatment of drugs and radiation. In the second part of the thesis, we explored a complementary aspect of chemical inhibition through CRISPR-mediated gene silencing of target genes and assessed its impact on the response to PRMT inhibition during radiotherapy. In the final part, we focused on elucidating the collective effects of a chemical inhibitor specifically targeting PRMT Type-I in combination with radiation. The resulting transcriptomic changes were analyzed using RNA sequencing, providing insights into the intricate details of how PRMT inhibition shapes the response to radiotherapy.

In the context of examining the alone effects of PRMT-targeted drugs on U373 cells, our findings unveiled a significant reduction of approximately 50% in the colony-forming capacity of U373 GBM cells after 24-hour incubation with the MS023 drug, in comparison to the control, throughout the 14-day colony-formation period. In contrast, no significant change was observed with SGC707, while LLY283 exhibited a substantial decrease of over 90% compared to the control **(Figure 3.2.2).** Our assessment also included primary cells, which demonstrated similar trends, emphasizing the potential clinical relevance of our findings. In the comparison between established U87MG cells and primary GBM4 cells, all GBM cell lines exhibited similar sensitivity to LLY283. However, GBM4 did not demonstrate sensitivity to MS023, suggesting a potential higher resistance in these cells (**Figure 3.2.1)**.

Investigating the use of PRMT inhibitors in GBM, studies have delved into their impact in the literature. For example, Sachamitr et al. (2021) found that LLY283 demonstrated a reduction in proliferation and self-renewal in patient-derived Glioma Stem Cells (GSCs). Another crucial finding was the efficient penetration of LLY-283 through the BBB, providing significant survival benefits in mice with orthotopic patient-derived GBM xenografts. This finding is particularly noteworthy as many new drugs for GBM often face challenges in clinical research due to limited BBB penetration. In another study by Liao et al. (2022), the PRMT3 selective inhibitor SGC707 exhibited a significant inhibitory effect on cell growth in U251 and U87 GBM cell lines, as well as in GSCs. Importantly, this inhibitory effect was not observed in normal brain glial cell lines, HEB and HMO6. It is worth noting that studies on MS023 and MS049 in GBM cells have not been encountered, necessitating further investigation.

Then, the impact of PRMT inhibitors on the radiation response was investigated in this study. Optimizing the pre-treatment incubation period before ionizing radiation enabled the examination of cooperative effects. A 24-hour pre-treatment with LLY283 and MS023 at specified doses effectively reduced cell growth, whereas MS049 and SGC707 alone did not exhibit a reduction in growth in the absence of radiation. When analyzing the results in conjunction with radiation, a lower colony formation ability was observed for MS023 and LLY283 compared to the control group (**Figure 3.3.1)**. With a 48-hour pretreatment, LLY283

displayed its toxicity, aligning with previous observations, and the number of colonies significantly decreased compared to the control group, even in the absence of radiation. While MS023 did not exhibit toxicity on its own, it demonstrated a noteworthy reduction in cell growth when combined with 4 Gy of radiation, surpassing the impact of either treatment alone. No significant difference was observed for MS049 and SGC707 when compared to the control group (**Figure 3.3.2).** After a 72-hour incubation, a significant decrease in proliferation for all drugs was observed following radiation treatment **(Figure 3.3.3)**. However, considering the initiation of the 14-day long-term clonogenic experiment with a limited number of cells, concerns arose regarding extended incubation with the drug. Consequently, for subsequent optimal experiments, it was decided to continue after a 48-hour drug incubation followed by 4 Gy radiation.

Our findings reveal a significant enhancement in the response of U373 cells to radiation with the use of MS023. Indeed, the literature currently has limited studies specifically on the impact of MS023 in glioblastoma cells. One such study, conducted by Samuel et al. (2018), demonstrates that MS023 reduces cell viability in U87 cells. Furthermore, upon reviewing the existing cancer research literature, there is also a noticeable absence of comprehensive studies examining the relationship between MS023 and radiotherapy. In the broader context of cancer studies, MS023 has exhibited notable potential in inhibiting type-I PRMT, resulting in the induction of interferon (IFN) responses and demonstrating potent antitumor activity against triple-negative breast tumors (Wu et al., 2021). Moreover, the combination of MS023 with immune therapy has shown promising results, leading to a significant reduction in the growth of triple-negative breast tumors (Zhang et al., 2023). Additionally, MS023 has been explored in the context of multiple myeloma, indicating its potential to induce cell cycle arrest and trigger cell death, emphasizing its significance in diverse cancer therapeutic approaches (Nguyen et al., 2023).

To study the effect of PRMT inhibition in the radiation response of GBM using a complementary genetic approach, we employed the CRISPR/Cas9 system to silence the expression of PRMT encoding genes. For this purpose, gRNAs for PRMT1, 3, 5, 6, and 8 were designed. The radiation response of cell lines generated with these gRNAs has also been investigated. Results indicated that gene reduction for PRMT6 and 8 could not be validated

via qPCR, and no combinational effect with radiation was observed. Notably, the depletion of PRMT6 was considered significant and warrants further exploration. This perspective is supported by a comparative study conducted by Huang et al. (2021), PRMT6 depletion in GSCs induced G1-phase arrest, reduced G2/M phase, and decreased methylation of chromatin condensation 1 (RCC1) that resulted in increased mitotic defects rendering the cells more sensitive to radiation.

PRMT1 is up-regulated in human glioma tissues, and studies on the functional role of PRMT1 in gliomas are limited. The investigation conducted by Wang et al. (2012) elucidated notable G1-S phase arrest, suppressed proliferation, and induced apoptosis in PRMT1 knockout GBM cell lines (T98G, U87MG, U251, and A172). Our results are consistent with these observations, highlighting a substantial decrease in proliferation and growth in PRMT1 knockout cells. Additionally, we observed a diminished colony formation capacity when PRMT1 knockout cells were subjected radiation treatment **(Figure 3.4.1)**.

Our findings indicate that there was no significant change in the survival potential of the PRMT3 knockout groups compared to the control group. Importantly, when radiation was combined, a noteworthy reduction in proliferation was observed in the PRMT3 KO received 2 Gy cells, confirming our expectations **(Figure 3.4.2)**. However, the study conducted by Liao et al. (2022) showed that the knockdown of PRMT3 led to a significant reduction in cell growth and proliferation in both GBM cells and GCSs. Additionally, they concluded that PRMT3 loss-of-function induces mitotic disruption and apoptosis in GBM cells. Their transcriptomic profiling also showed that PRMT3 knockdown cells had downregulation of HIF1A along with glycolytic pathway genes in GBM cells. Notably, HIF-1 expression was upregulated in glioblastoma and modulated a set of signaling pathways to cause profound effects on the response of cancer to radiotherapy (Huang et al. 2020).

MS023 targets numerous proteins, including PRMT1, 3, 4, 6, and 8, yet individual knockouts of PRMT did not replicate the observed phenotypic effects of chemical interventions. Despite generating a PRMT1 knockout cell line, its cellular survival was significantly affected, suggesting the potential application of inducible gene ablation. Our primary plans involve generating stable U373 cell lines with PRMT6 and PRMT8 knockout, aiming to investigate their responses to radiotherapy. Additionally, establishing stable cell lines with the depletion

of multiple PRMT genes would complement MS023. Future studies may explore the comprehensive impact of simultaneously knocking out multiple PRMTs to elucidate potential synergies or compensatory mechanisms. Future directions also encompass the re-examination and analysis of transcriptomic changes in a genetic ablation-based scenario that mimics the phenotypic response of MS023.

Subsequently, in light of the synergistic effect of MS023 in combination with radiation in our thesis, we conducted a transcriptomic changes analysis. RNA sequencing allows for the assessment of transcriptomic changes in cells, especially those subjected to treatment. The analysis results enable us to comment on differentially expressed genes and distinguish pathways through Gene Set Enrichment Analysis.

To investigate the impact of type-I PRMT inhibition on transcriptomic changes in U373 GBM cells, cells treated with 48h MS023 followed by 4 Gy radiation were compared with the control group. PCA analysis revealed distinct clustering patterns among triplicate samples, indicating significant changes in gene expression profiles **(Figure 3.5.1.1)**. Subsequently, through a detailed analysis, we identified 7189 differentially expressed genes following MS023 treatment, comprising 3570 upregulated and 3619 downregulated genes. Differential gene expression is a critical aspect of comprehending the influence of MS023 on cellular processes. Consistently, GSEA revealed that the G2M Checkpoint, E2F Targets, and mitotic spindle genes were significantly downregulated, while the apoptosis-associated genes and hypoxia were upregulated after MS023 treatment.

Upon comparing the samples subjected to 4 Gy radiation with the control group, a total of 230 genes exhibited differential expression, with 85 of them being downregulated and 145 upregulated **(Figure 3.5.2.1)**. Consistently, GSEA revealed that the cell cycle process and cell division genes were significantly downregulated. Conversely, genes associated with the negative regulation of cell population proliferation were upregulated after radiation treatment. These findings suggest a targeted impact on key cellular processes, providing insights into the molecular mechanisms influenced by radiation in the examined context.

The subsequent analysis of MS023 treatment unveiled a profound influence on the cellular landscape, characterized by a significant number of differentially expressed genes. This suggests that MS023 exerts a broad and intricate impact within the cell, affecting various

molecular processes. Adding a layer of surprise to these findings is the comparison with irradiation, which unexpectedly led to fewer gene expressions in the cell. Unraveling these dynamics holds the potential to provide valuable insights into the intricate interplay between PRMT inhibition, radiation response, and the broader cellular transcriptional landscape.

Subsequently, the combinatorial treatment of MS023 and 4 Gy in U373 GBM cells, demonstrating a synergistic effect in cell viability and proliferation results, was compared with the control group. The combination treatment significantly altered the expression of 7125 differentially expressed genes, with 3589 upregulated and 3536 downregulated genes. GSEA highlighted changes in pathways, revealing the downregulation of E2F targets and G2M checkpoints and DNA repair, and the upregulation of apoptosis, UV response, and hypoxia pathways. These findings collectively deepen our understanding of how MS023, both individually and in combination with radiation, orchestrates complex molecular changes, providing valuable insights for potential therapeutic applications (**Figure 4).**

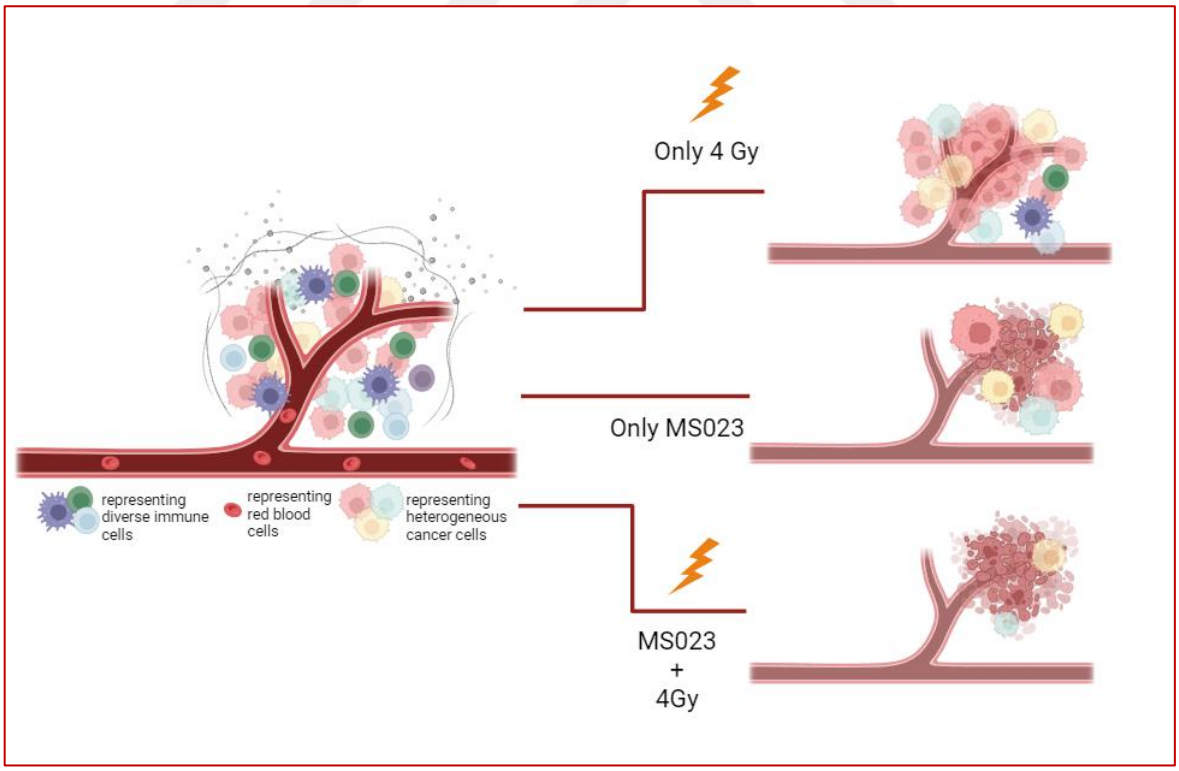

Figure 4. Radiosensitization of GBM with combinational treatment of MS023 and IR

In summary, our observations indicate that PRMT inhibition significantly enhances the radiation response in GBM cells. The in-depth transcriptomic analysis conducted for a comprehensive exploration of this effect revealed that MS023 upregulates apoptosis and hypoxia-related genes in U373 cells, thereby enhancing their response to radiation. Additionally, the downregulation of cell cycle-regulated and G2M cell checkpoint genes suggests a potential slowdown or cessation of cell proliferation and growth following IR-induced DNA damage. As a continuation of this thesis, we aim to strengthen our hypothesis through experiments focusing on cell cycle and apoptosis-related investigations to validate these results.

The phosphorylation of H2AX is a well-characterized marker for DNA damage. γH2AX functions as a signal to recruit repair proteins to the site of the break, facilitating the repair of damaged DNA. Additionally, the detection and quantification of γH2AX levels are used in research to assess the extent of DNA damage and the efficacy of DNA repair mechanisms. Our findings indicate that only radiation treatment led to a significantly higher level of γH2AX at the end of the first hour for control group. Conversely, the level of γH2AX is a rapidly changing factor, and we observed that PRMT inhibition resulted in less activated H2AX at the end of the first hour after radiation **(Figure 3.6)**. In our RNA sequencing results, we observed that cells treated with MS023 exhibited downregulation of DNA damage-related genes. To correlate these findings, further experimentation involving various DNA damage response-related assays would be beneficial for the overall advancement of the study.

Future Directions

The exploration of a complementary study that precisely replicates the effects of MS023 through genetic ablation holds significant scientific value and adds uniqueness to this research. Additionally, our laboratory-generated radioresistant cell line serves as a suitable platform to rigorously test the inhibitory effects of PRMT in the context of MS023. Ongoing experiments, focusing on MS023-induced pathways, will be meticulously completed, and a series of experiments will continue to explore genes related to cell cycle and division. This comprehensive research strategy aims to significantly enhance our understanding of the complex molecular mechanisms underlying the synergistic reduction in cellular proliferation observed with combined treatment. Furthermore, detailed investigations into the molecular

effects of MS023-induced pathways are crucial, emphasizing a comprehensive understanding of the cellular response. In-depth exploration of specific gene alterations related to cell cycle and division will provide nuanced insights into the molecular foundations of the observed reduction in cellular proliferation. Lastly, illuminating the complex cellular pathways modulated by MS023 in the context of radiotherapy and testing these effects in a clinically relevant orthotopic *in vivo* model will not only validate our findings but also shed light on the potential translational applications of this combined treatment strategy.

REFERENCES

Ali, M. Y., et al. (2020). "Radioresistance in Glioblastoma and the Development of Radiosensitizers." Cancers 12(9): 2511.

Alimohammadi, E., et al. (2020). "The impact of extended adjuvant temozolomide in newly diagnosed glioblastoma multiforme: a meta-analysis and systematic review." Oncology Reviews 14(1).

Barani, I. J., & Larson, D. A. (2015). Radiation therapy of glioblastoma. Current understanding and treatment of gliomas, 49-73.

Bartkova B., Jr., Hořejší Z., Koed K., Krämer A., Tort F., Zieger K., Guldberg P., Sehested M., Nesland J.M., Lukas C., et al. DNA damage response as a candidate anti-cancer barrier in early human tumorigenesis. Nat. Cell Biol. 2005;434:864–870.

Biau, J., Chautard, E., Verrelle, P., & Dutreix, M. (2019). Altering DNA repair to improve radiation therapy: specific and multiple pathway targeting. Frontiers in oncology, 9, 1009.

Bird, A. W., Yu, D. Y., Pray-Grant, M. G., Qiu, Q., Harmon, K. E., Megee, P. C., . . . Christman, M. F. (2002). Acetylation of histone H4 by ESA1 is required for DNA double-strand break repair. Nature, 419(6905), 411-415. doi:10.1038/nature01035

Biterge, B. (2016). A mini review on post-translational histone modifications. MOJ Cell Science & Report, 3(1), 1-4.

Celeste, A., Difilippantonio, S., Difilippantonio, M. J., Fernandez-Capetillo, O., Pilch, D. R., Sedelnikova, O. A., . . . Nussenzweig, A. (2003). H2AX haploinsufficiency modifies genomic stability and tumor susceptibility. Cell, 114(3), 371-383. doi:10.1016/s0092-8674(03)00567-1

Celeste, A., Fernandez-Capetillo, O., Kruhlak, M. J., Pilch, D. R., Staudt, D. W., Lee, A., . . . Nussenzweig, A. (2003). Histone H2AX phosphorylation is dispensable for the initial recognition of DNA breaks. Nature Cell Biology, 5(7), 675-679. doi:10.1038/ncb1004

Coster, G., & Goldberg, M. (2010). The cellular response to DNA damage: a focus on MDC1 and its interacting proteins. Nucleus, 1(2), 166-178.Goldberg, M., Stucki, M., Falck, J., D'Amours, D., Rahman, D., Pappin, D., . . . Jackson, S. P. (2003). MDC1 is required for the intra-s-phase DNA damage checkpoint. Nature, 421(6926), 952-956. doi:10.1038/nature01445

Deckbar, D., Jeggo, P. A., & Löbrich, M. (2011). Understanding the limitations of radiation-induced cell cycle checkpoints. Critical reviews in biochemistry and molecular biology, 46(4), 271-283.

Fernandes, C., Costa, A., Osório, L., Lago, R. C., Linhares, P., Carvalho, B., & Caeiro, C. (2017). Current standards of care in glioblastoma therapy. Exon Publications, 197-241.

Goenka, A., Tiek, D., Song, X., Huang, T., Hu, B., & Cheng, S. Y. (2021). The many facets of therapy resistance and tumor recurrence in glioblastoma. Cells, 10(3), 484.

Gomez Godinez, V., Kabbara, S., Sherman, A., Wu, T., Cohen, S., Kong, X., ... & Berns, M. W. (2020). DNA damage induced during mitosis undergoes DNA repair synthesis. PloS one, 15(4), e0227849.

Gong, F., & Miller, K. M. (2013). Mammalian DNA repair: Hats and hdacs make their mark through histone acetylation. Mutation Research/Fundamental and Molecular Mechanisms of Mutagenesis, 750(1-2), 23-30. doi:10.1016/j.mrfmmm.2013.07.002

Gong, F., Clouaire, T., Aguirrebengoa, M., Legube, G., & Miller, K. M. (2017). Histone demethylase KDM5A regulates the ZMYND8–NuRD chromatin remodeler to promote DNA repairKDM5A promotes DNA repair via ZMYND8–NuRD. The Journal of cell biology, 216(7), 1959-1974.

Gray, G. K., McFarland, B. C., Nozell, S. E., & Benveniste, E. N. (2014). NF-κB and STAT3 in glioblastoma: therapeutic targets coming of age. Expert review of neurotherapeutics, 14(11), 1293-1306.

Grunstein, M. Histone acetylation in chromatin structure and transcription. Nature 389, 349–352 (1997). https://doi.org/10.1038/38664

Hanif, F., Muzaffar, K., Perveen, K., Malhi, S. M., & Simjee, S. U. (2017). Glioblastoma multiforme: a review of its epidemiology and pathogenesis through clinical presentation and treatment. Asian Pacific journal of cancer prevention: APJCP, 18(1), 3.

Hanks, S. K., Rodriguez, L. V., & Rao, P. N. (1983). Relationship between histone phosphorylation and premature chromosome condensation. *Experimental cell research*, 148(2), 293-302.

Huang, R., & Zhou, P. K. (2020). HIF-1 signaling: A key orchestrator of cancer radioresistance. *Radiation Medicine and Protection*, *1*(1), 7-14.

Hunt, C. R., Ramnarain, D., Horikoshi, N., Iyengar, P., Pandita, R. K., Shay, J. W., & Pandita, T. K. (2013). Histone modifications and DNA double-strand break repair after exposure to ionizing radiations. Radiation research, 179(4), 383-392.

Hwang, J. W., Cho, Y., Bae, G. U., Kim, S. N., & Kim, Y. K. (2021). Protein arginine methyltransferases: Promising targets for cancer therapy. *Experimental & molecular medicine*, *53*(5), 788-808.

Jacquet, K., Fradet-Turcotte, A., Avvakumov, N., Lambert, J., Roques, C., Pandita, R., . . . Côté, J. (2016). The tip60 complex regulates bivalent chromatin recognition by 53BP1 through direct h4k20me binding and H2AK15 acetylation. Molecular Cell, 62(3), 409-421. doi:10.1016/j.molcel.2016.03.031

Jeon H.-Y., Ham S.W., Kim J.-K., Jin X., Lee S.Y., Shin Y.J., Choi C.-Y., Sa J.K., Kim S.H., Chun T., et al. Ly6G+ inflammatory cells enable the conversion of cancer cells to cancer stem cells in an irradiated glioblastoma model. Cell Death Differ. 2019;26:2139–2156. doi: 10.1038/s41418-019-0282-0.

Joubert, A., & Foray, N. (2006). Repair of radiation-induced DNA double-strand breaks in human cells: history, progress and controversies. *New research on DNA repair*.

Kaidi, A., & Jackson, S. P. (2013). KAT5 tyrosine phosphorylation couples chromatin sensing to ATM signalling. *Nature*, *498*(7452), 70-74.

Karakaidos, P., Karagiannis, D., & Rampias, T. (2020). Resolving DNA Damage: Epigenetic regulation of DNA repair. Molecules, 25(11), 2496. Mao, Z., Bozzella, M., Seluanov, A., & Gorbunova, V. (2008). Comparison of nonhomologous end joining and homologous recombination in human cells. DNA repair, 7(10), 1765-1771.

Kim S.-H., Joshi K., Ezhilarasan R., Myers T.R., Siu J., Gu C., Nakano-Okuno M., Taylor D., Minata M., Sulman E.P., et al. EZH2 Protects Glioma Stem Cells from Radiation-Induced Cell Death in a MELK/FOXM1-Dependent Manner. Stem Cell Rep. 2015;4:226–238. doi: 10.1016/j.stemcr.2014.12.006.

Li, R., Wang, H., Liang, Q., Chen, L., & Ren, J. (2022). Radiotherapy for glioblastoma: clinical issues and nanotechnology strategies. Biomaterials Science, 10(4), 892-908.

Liao, Y., Luo, Z., Lin, Y., Chen, H., Chen, T., Xu, L., ... & Lu, Q. R. (2022). PRMT3 drives glioblastoma progression by enhancing HIF1A and glycolytic metabolism. *Cell Death & Disease*, *13*(11), 943.

Liu H., Sun Y., Qi X., Gordon R.E., O'Brien J.A., Yuan H., Zhang J., Wang Z., Zhang M., Song Y., et al. EZH2 Phosphorylation Promotes Self-Renewal of Glioma Stem-Like Cells Through NF-κB Methylation. Front. Oncol. 2019;9:641. doi: 10.3389/fonc.2019.00641.

Maachani, U. B., Shankavaram, U., Kramp, T., Tofilon, P. J., Camphausen, K., & Tandle, A. T. (2016). FOXM1 and STAT3 interaction confers radioresistance in glioblastoma cells. Oncotarget, 7(47), 77365.

Marampon, F., Gravina, G. L., Zani, B. M., Popov, V. M., Fratticci, A., Cerasani, M., ... & Festuccia, C. (2014). Hypoxia sustains glioblastoma radioresistance through ERKs/DNA-PKcs/HIF-1α functional interplay. *International journal of oncology*, *44*(6), 2121-2131.

Minniti, G., Muni, R., Lanzetta, G., Marchetti, P., & Enrici, R. M. (2009). Chemotherapy for glioblastoma: current treatment and future perspectives for cytotoxic and targeted agents. Anticancer research, 29(12), 5171-5184.

Ogiwara, H., Ui, A., Otsuka, A., Satoh, H., Yokomi, I., Nakajima, S., . . . Kohno, T. (2011). Histone acetylation by CBP and P300 at double-strand break sites facilitates SWI/SNF chromatin remodeling and the recruitment of non-homologous end joining factors. Oncogene, 30(18), 2135-2146. doi:10.1038/onc.2010.592

Ostrom, Q. T., Price, M., Neff, C., Cioffi, G., Waite, K. A., Kruchko, C., & Barnholtz-Sloan, J. S. (2022). CBTRUS statistical report: primary brain and other central nervous system tumors diagnosed in the United States in 2015–2019. Neuro-oncology, 24(Supplement_5), v1-v95.

Ou, A., Yung, W. A., & Majd, N. (2020). Molecular mechanisms of treatment resistance in glioblastoma. International journal of molecular sciences, 22(1), 351.

Parsons, D. W., Jones, S., Zhang, X., Lin, J. C. H., Leary, R. J., Angenendt, P., ... & Kinzler, K. W. (2008). An integrated genomic analysis of human glioblastoma multiforme. science, 321(5897), 1807-1812.

Pei, H., Zhang, L., Luo, K., Qin, Y., Chesi, M., Fei, F., ... & Lou, Z. (2011). MMSET regulates histone H4K20 methylation and 53BP1 accumulation at DNA damage sites. Nature, 470(7332), 124-128.

Pilié, P. G., Tang, C., Mills, G. B. & Yap, T. A. State-of-the-art strategies for targeting the DNA damage response in cancer. Nat. Rev. Clin. Oncol. 16, 81–104 (2019).

Qi, W., Yan, L., Liu, C., Fu, R., Wang, H., & Shao, Z. (2016). Abnormal histone acetylation of CD8+ T cells in patients with severe aplastic anemia. International journal of hematology, 104(5), 540-547.

Ran, F. A., Hsu, P. D., Wright, J., Agarwala, V., Scott, D. A., & Zhang, F. (2013). Genome engineering using the CRISPR-Cas9 system. Nature protocols, 8(11), 2281-2308.

Reisz, J. A., Bansal, N., Qian, J., Zhao, W., & Furdui, C. M. (2014). Effects of ionizing radiation on biological molecules—mechanisms of damage and emerging methods of detection. *Antioxidants & redox signaling*, *21*(2), 260-292.

Ren, J., Xu, B., Ren, J., Liu, Z., Cai, L., Zhang, X., ... & Ding, L. (2023). The Importance of M1-and M2-Polarized Macrophages in Glioma and as Potential Treatment Targets. Brain Sciences, 13(9), 1269.

Rogakou, E. P., Boon, C., Redon, C., & Bonner, W. M. (1999). Megabase chromatin domains are involved in DNA double-strand breaks in vivo. Journal of Cell Biology, 146(5), 905-916. doi:10.1083/jcb.146.5.905

Samuel, S. F., Marsden, A. J., Deepak, S., Rivero, F., Greenman, J., & Beltran-Alvarez, P. (2018). Inhibiting arginine methylation as a tool to investigate cross-talk with methylation and acetylation post-translational modifications in a glioblastoma cell line. *Proteomes*, *6*(4), 44.

Singh, R., Lehrer, E. J., Wang, M., Perlow, H. K., Zaorsky, N. G., Trifiletti, D. M., ... & Palmer, J. D. (2021). Dose escalated radiation therapy for glioblastoma multiforme: an international systematic review and meta-analysis of 22 prospective trials. International Journal of Radiation Oncology* Biology* Physics, 111(2), 371-384.

Stewart, G. S., Wang, B., Bignell, C. R., Taylor, A. M., & Elledge, S. J. (2003). MDC1 is a mediator of the mammalian DNA damage checkpoint. Nature, 421(6926), 961-966. doi:10.1038/nature01446

Stupp, R., Mason, W. P., Van Den Bent, M. J., Weller, M., Fisher, B., Taphoorn, M. J., ... & Mirimanoff, R. O. (2005). Radiotherapy plus concomitant and adjuvant temozolomide for glioblastoma. New England journal of medicine, 352(10), 987-996.

Tang, J., Cho, N., Cui, G. et al. Acetylation limits 53BP1 association with damaged chromatin to promote homologous recombination. Nat Struct Mol Biol 20, 317–325 (2013).

Wang J., Cheng P., Pavlyukov M.S., Hongyu L., Zhang Z., Kim S.-H., Minata M., Mohyeldin A., Xie W., Chen D., et al. Targeting NEK2 attenuates glioblastoma growth and radioresistance by destabilizing histone methyltransferase EZH2. J. Clin. Investig. 2017;127:3075–3089. doi: 10.1172/JCI89092.

Wei, S., Li, C., Yin, Z., Wen, J., Meng, H., Xue, L., & Wang, J. (2018). Histone methylation in DNA repair and clinical practice: new findings during the past 5 years. Journal of Cancer, 9(12), 2072.

Wen, J., Chen, W., Zhu, Y., & Zhang, P. (2021). Clinical features associated with the efficacy of chemotherapy in patients with glioblastoma (GBM): a surveillance, epidemiology, and end results (SEER) analysis. *BMC cancer*, *21*, 1-10.

Womeldorff, M., Gillespie, D., & Jensen, R. L. (2014). Hypoxia-inducible factor–1 and associated upstream and downstream proteins in the pathophysiology and management of glioblastoma. Neurosurgical focus, 37(6), E8.

Wu, W., Klockow, J. L., Zhang, M., Lafortune, F., Chang, E., Jin, L., ... & Daldrup-Link, H. E. (2021). Glioblastoma multiforme (GBM): An overview of current therapies and mechanisms of resistance. Pharmacological Research, 171, 105780.

Xiao, C., Fan, T., Tian, H., Zheng, Y., Zhou, Z., Li, S., ... & He, J. (2021). H3K36 trimethylation-mediated biological functions in cancer. Clinical epigenetics, 13(1), 1-19.